



BNL-91287-2010

Formalism for neutron cross section
covariances in the resonance region
using kernel approximation

P. Oblozinsky, Y.-S. Cho*, C.M. Mattoon, S.F. Mughabghab

National Nuclear Data Center, Brookhaven National Laboratory
Upton, New York, 11973 - 5000, U.S.A.

* *On sabbatical leave from Nuclear Data Evaluation Lab, KAERI, Korea*

April 9, 2010

National Nuclear Data Center
Brookhaven National Laboratory
P.O. Box 5000
Upton, NY 11973-5000
www.bnl.gov

Notice: This manuscript has been authored by employees of Brookhaven Science Associates, LLC under Contract No. DE-AC02-98CH10886 with the U.S. Department of Energy. The publisher by accepting the manuscript for publication acknowledges that the United States Government retains a non-exclusive, paid-up, irrevocable, world-wide license to publish or reproduce the published form of this manuscript, or allow others to do so, for United States Government purposes.

DISCLAIMER

This report was prepared as an account of work sponsored by an agency of the United States Government. Neither the United States Government nor any agency thereof, nor any of their employees, nor any of their contractors, subcontractors, or their employees, makes any warranty, express or implied, or assumes any legal liability or responsibility for the accuracy, completeness, or any third party's use or the results of such use of any information, apparatus, product, or process disclosed, or represents that its use would not infringe privately owned rights. Reference herein to any specific commercial product, process, or service by trade name, trademark, manufacturer, or otherwise, does not necessarily constitute or imply its endorsement, recommendation, or favoring by the United States Government or any agency thereof or its contractors or subcontractors. The views and opinions of authors expressed herein do not necessarily state or reflect those of the United States Government or any agency thereof..

Formalism for neutron cross section covariances in the resonance region using kernel approximation

P. Obložinský, Y.-S. Cho^{*)}, C.M. Mattoon, S.F. Mughabghab

National Nuclear Data Center, Brookhaven National Laboratory
Upton, New York, 11973 – 5000, U.S.A.

^{*)} On sabbatical leave from Nuclear Data Evaluation Lab, KAERI, Korea

April 9, 2010

Notice: This manuscript has been authored by employees of Brookhaven Science Associates, LLC under Contract No. DE-AC02-98CH10886 with the U.S. Department of Energy. The publisher by accepting the manuscript for publication acknowledges that the United States Government retains a non-exclusive, paid-up, irrevocable, world-wide license to publish or reproduce the published form of this manuscript, or allow others to do so, for United States Government purposes.

Abstract

We describe analytical formalism for estimating neutron radiative capture and elastic scattering cross section covariances in the resolved resonance region. We use capture and scattering kernels as the starting point and show how to get average cross sections in broader energy bins, derive analytical expressions for cross section sensitivities, and deduce cross section covariances from the resonance parameter uncertainties in the recently published Atlas of Neutron Resonances. The formalism elucidates the role of resonance parameter correlations which become important if several strong resonances are located in one energy group. Importance of potential scattering uncertainty as well as correlation between potential scattering and resonance scattering is also examined. Practical application of the formalism is illustrated on $^{55}\text{Mn}(n,\gamma)$ and $^{55}\text{Mn}(n,\text{el})$.

Contents

1	Introduction	1
2	Average cross sections from kernels	4
2.1	Radiative capture	4
2.2	Elastic scattering	6
2.2.1	Low energy approximation	7
2.2.2	Approximations at higher energies	9
2.2.3	Role of outside resonances	10
3	Covariances for a single resonance	11
3.1	Radiative capture	11
3.1.1	Computation directly from kernels	11
3.1.2	Computation from resonance parameters	12
3.2	Elastic scattering	16
3.2.1	Resonance contribution	16
3.2.2	Potential scattering contribution	19
4	Covariances for many resonances	21
4.1	Formalism for many resonances	21
4.2	Explicit treatment of two resonances	22
4.2.1	Capture computed directly from kernels	22
4.2.2	Capture computed from resonance parameters	23
4.2.3	Elastic scattering	25
5	Covariances in thermal energy range	26
5.1	Thermal radiative capture	26
5.2	Thermal elastic scattering	27
5.2.1	Thermal scattering cross section uncertainty	27

5.2.2	Impact of scattering radius uncertainty	28
6	Correlation coefficients	30
6.1	Notation	30
6.2	Transmission and capture measurements	31
6.3	Default values of correlation coefficients	32
6.3.1	Single resonance	33
6.3.2	Resonance - resonance	34
6.3.3	Potential scattering - resonance scattering	34
6.3.4	Energy bin - energy bin	35
6.3.5	Thermal region - resonance region	35
6.3.6	Cross-correlations	36
7	Resonance covariance module in EMPIRE	37
7.1	Functionalities	37
7.2	Evaluation procedure	38
8	Application to ^{55}Mn	41
8.1	^{55}Mn uncertainty data in Atlas	42
8.1.1	Thermal values	42
8.1.2	Resonance values	43
8.2	$^{55}\text{Mn}(n,\gamma)$ covariances	46
8.2.1	Energy binning	46
8.2.2	Uncertainties for capture	48
8.2.3	Covariances for capture	49
8.3	$^{55}\text{Mn}(n,\text{el})$ covariances	51
8.3.1	Energy binning	51
8.3.2	Uncertainties for elastic scattering	52
8.3.3	Covariances for elastic scattering	54
8.4	Comparison with MF32	56
8.4.1	Evaluation procedure	56
8.4.2	Results and discussion	57
8.5	Comparison with ENDF/A	61
8.5.1	$^{55}\text{Mn}(n,\gamma)$ uncertainties	61
8.5.2	$^{55}\text{Mn}(n,\text{el})$ uncertainties	63
8.6	Final results	63
8.6.1	Adopted correlation coefficients	63
8.6.2	Quality assurance	64

9 Conclusions	68
Bibliography	70

Chapter 1

Introduction

Our goal is to resolve continuing issues with neutron cross section covariances in the resolved resonance region. These issues were discussed at several recent US nuclear reaction data meetings, notably the Covariance Workshop in Port Jefferson 2008, Mini-CSEWG Meeting in Port Jefferson 2009 and CSEWG Meeting in BNL 2009. Of these issues probably the most important is the decline of uncertainties observed after collapsing covariances into multigroup representations. This decline, caused by the lack of medium- and long-range correlations, is deemed to be unphysical. The other issues include unrealistically low uncertainties claimed by some evaluators, adjustment of thermal cross section uncertainties to get agreement with resonance parameter uncertainties, proper inclusion of scattering radius uncertainty and discrepancies between the major processing codes NJOY and PUFF in processing resonance parameter covariances (MF32 file).

The present work attempts to find a solution to these issues by developing a transparent formalism for cross section covariances (MF33 file) based on resonance parameter uncertainties of Atlas of Neutron Resonances [1]. The idea is to derive suitable analytical expressions that would provide sufficient insight for propagating resonance parameter uncertainties into cross section uncertainties. This should be done for a single resonance located in one energy group (bin), and also for several resonances in one energy group (bin) in order to fully understand and prevent decline of cross section uncertainties in collapsing. The full covariance matrix will be constructed with a thermal region based directly on experimental data, avoiding the adjustment issue; scattering radius uncertainty will be handled explicitly, and by using MF33 representation we would bypass MF32 processing issue.

In the past we have already attempted to derive and analyze analytical expressions in the resonance region by looking into detailed energy dependencies for capture [2]. This appeared to be not very practical since the resonance widths are in general much smaller than a width of typical energy bin in multigroup representations. Thus, even though we have seen fine details, we failed to get sufficient understanding on the multigroup level.

In view of this the present work starts with kernels which properly reflect strength of resonances and are thus suitable for characterizing cross sections over broader energy bins. The inspiration came from S. Mughabghab [3] who was using kernels in his quick estimates of uncertainties. The details of the procedure, however, were not fully documented. Therefore, we decided to work out rigorous mathematical procedures that would reveal all details and avoid future confusion.

Before we proceed with developing actual formalism, several comments should be made.

Not unexpectedly, in the course of the present work it was found out that the idea of using kernels for obtaining capture (and fission) cross section covariances in the resonance region is not new. It has been originally proposed by J.D. Smith III in 1980 [4] and since then it has been used in processing of MF32 files both by NJOY and PUFF. Since PUFF is using analytical expressions for sensitivities we could check our own expressions derived for capture with those given in PUFF-IV Manual [5].

The situation with elastic scattering is more complicated due to interference effects and presence of potential scattering. Neither NJOY nor PUFF use the scattering kernel in processing and the PUFF manual does not offer analytical expressions for sensitivities. However, following S. Mughabghab's procedure for estimating elastic scattering cross section uncertainties, we use scattering kernel as the starting point for computing group cross section even though it represents an approximation which is less robust than in the case of capture.

It appears that the kernel approximation to infer covariances has also been used by Fritz Fröhner in early 1990s. Fröhner applied analysis of resonance areas of transmission and capture data in order to evaluate resonance parameters (MF2 file) and resonance parameter covariances (MF32 file) for structural materials [6, 7, 8].

Starting from resonance areas of transmission dips ($A \pm \Delta A$) and capture peaks ($A_\gamma \pm \Delta A_\gamma$) he deduced neutron and radiative widths ($\Gamma_n \pm \Delta \Gamma_n, \Gamma_\gamma \pm \Delta \Gamma_\gamma$) and produced MF2 and MF32 files for ^{56}Fe and ^{60}Ni . However, only MF2 was included in JEFF-3 library, while MF32 including proposed scattering radius uncertainty extension of ENDF-6 format appear to have been lost. We propose to proceed in reversed order. We would start with resonance parameter uncertainties and infer resonance areas (kernels) uncertainties which are proportional to cross section uncertainties.

The report is organized as follows. In Chapter 2 we derive expressions for average cross sections using capture and scattering kernels. In Chapters 3-5 we describe formalism for uncertainties of average cross sections, starting from a single resonance in Chapter 3, followed by many resonances in Chapter 4 and complemented by thermal region in Chapter 5. Then, in Chapter 6 we discuss correlation coefficients. This new formalism was implemented in the resonance covariance module of the code EMPIRE as described in Chapter 7. Chapter 8 is devoted to a sample case, ^{55}Mn capture and elastic scattering. Conclusions are given in Chapter 9.

Chapter 2

Average cross sections from kernels

The starting point in development of our formalism is a suitable description of the average cross section for a single resonance. The average, even if done over relatively broad energy interval compared to the width of the resonance, should preserve reasonable degree of the resonance individuality, yet considerably simplify its treatment. While averaging should be avoided if a detailed description of resonance cross sections is required, it should be adequate for producing covariances on the group level required by most applications.

2.1 Radiative capture

For simplicity we restrict ourselves to single-level Breit-Wigner (SLBW) formalism. This is sufficiently representative for our purposes and relatively easy to implement analytically. We first discuss a single resonance in one energy group, then proceed with several resonances in one group. For the moment, we consider non-fissile materials, provide expressions for capture cross sections. We also note that the expressions for fission cross sections can be obtained by straightforward modification - replacing radiative width with fission width and adding fission width to total resonance width.

For a single resonance of the energy E_0 , at the neutron incident energy E , the capture cross section can be expressed by the Breit-Wigner formula as

$$\sigma_\gamma(E) = \pi\lambda^2 \frac{\Gamma_n \Gamma_\gamma}{(E - E_0)^2 + \frac{1}{4}\Gamma^2}, \quad (2.1)$$

where we dropped all indices related to quantum numbers. Here λ is the de Broglie wavelength of the incoming neutron,

$$\lambda = \frac{\hbar}{\sqrt{2mE}}, \quad (2.2)$$

m is the neutron reduced mass and \hbar the Planck constant. The spin statistical factor is given by

$$g = \frac{2J + 1}{2(2I + 2)}, \quad (2.3)$$

with J being the spin of the resonance and I the spin of the target nucleus. The total resonance width is given as

$$\Gamma = \Gamma_n + \Gamma_\gamma, \quad (2.4)$$

with Γ_n and Γ_γ being the neutron and radiative width, respectively. The resonance parameters, E_0, J, Γ_n and Γ_γ , along with their uncertainties can in principle be found in the Atlas of Neutron Resonances [1].

As a next step we compute the capture kernel which characterizes the strength of the resonance. The kernel is defined as integral

$$A_\gamma = \int_{-\infty}^{+\infty} \sigma_\gamma(E) dE, \quad (2.5)$$

which gives (Ref. [1], p.72, Eq. 3.4)

$$A_\gamma = 2\pi^2 \lambda^2 g \frac{\Gamma_n \Gamma_\gamma}{\Gamma}. \quad (2.6)$$

Considering an isolated resonance of the energy E_0 located in sufficiently broad group with the energy width

$$\Delta E = E_1 - E_2 \quad (2.7)$$

one can approximate the average cross section in this group using the capture kernel

$$\bar{\sigma}_\gamma = \frac{1}{\Delta E} \int_{E_2}^{E_1} \sigma_\gamma(E) dE \approx \frac{1}{\Delta E} \int_{-\infty}^{+\infty} \sigma_\gamma(E) dE = a \frac{g \Gamma_n \Gamma_\gamma}{\Gamma}, \quad (2.8)$$

which is our starting relation for deriving the formalism for covariances of average (group) capture cross sections. We simplify notation by introducing the quantity

$$a = \frac{2\pi^2 \lambda^2}{\Delta E}, \quad (2.9)$$

which has units of barn/eV and can be computed using the wave number defined as

$$k = \frac{1}{\lambda} = \frac{\sqrt{2mE}}{\hbar} = 2.19677 \times 10^{-3} \frac{A}{A+1} \sqrt{E}. \quad (2.10)$$

Here, the numerical constant, taken from NJOY manual yields k^2 in barns [9] (see p.III-9), A is the mass number and E is the neutron incident energy in eV. Then,

$$a = \frac{2\pi^2}{k^2} \frac{1}{\Delta E} = \frac{2\pi^2}{(2.197 \times 10^{-3})^2} \frac{(A+1)^2}{A^2} \frac{1}{E_0 \Delta E}$$

giving

$$a = 4.089 \times 10^6 \frac{(A+1)^2}{A^2} \frac{1}{E_0 \Delta E}, \quad (2.11)$$

which exhibits strong energy dependence on E_0 . This dependence can be largely omitted as long as we are discussing single resonances, but it will play an important role once we deal with many resonances in a single energy group.

2.2 Elastic scattering

Description of neutron elastic scattering requires a more complicated formalism since one has to add potential (hard-sphere) scattering and account for quantum-mechanical interference effects.

Following Fröhner [10], within the SLBW formalism the elastic scattering cross section for a single resonance can be expressed as

$$\sigma_n(E) = 4\pi\lambda^2(2l+1)\sin^2\phi_l + \pi\lambda^2 g \frac{\Gamma_n \Gamma \cos(2\phi_l) + 2(E-E_0)\Gamma_n \sin(2\phi_l)}{(E-E_0)^2 + \frac{1}{4}\Gamma^2}, \quad (2.12)$$

where ϕ_l is the phase shift

$$\phi_0 = kR', \quad (2.13)$$

$$\phi_l = kR' - \arctan(kR') \quad (2.14)$$

and R' is the scattering radius.

Eq. (2.12) has three terms. The 1st term describes potential scattering, which is nearly constant as a function of energy. The second term stands for the symmetric resonance cross section. The 3rd term, containing $2(E - E_0)\Gamma_n \sin(2\phi_l)$ in the numerator, describes interference between potential (hard-sphere) and resonance scattering which is negative at $E < E_0$ and positive at $E > E_0$. These negative and positive contributions are approximately equal and they cancel out if one computes the average elastic scattering cross section by integrating the cross section over a broad energy interval around the resonance energy E_0 .

Using the expression

$$\cos(2\phi_l) = 2 \cos^2 \phi_l - 1 = 1 - 2 \sin^2 \phi_l \quad (2.15)$$

one can re-write Eq. (2.12) into the form identical with that given in the ENDF-6 Formats Manual [11] (see p. 317)

$$\sigma_n(E) = 4\pi\lambda^2(2l + 1) \sin^2 \phi_l + \pi\lambda^2 g \frac{\Gamma_n^2 - 2\Gamma_n\Gamma \sin^2 \phi_l + 2(E - E_0)\Gamma_n \sin(2\phi_l)}{(E - E_0)^2 + \frac{1}{4}\Gamma^2}. \quad (2.16)$$

The following comment should be made. Strictly speaking, Eq. (2.16) given in ENDF-6 Manual [11] cannot be obtained from Eq. (2.12) provided by Fröhner. However, NJOY Manual (see Ref. [9], p. III-8) starts with a relation that differs somewhat from Eq. (2.12), instead of $\Gamma_n\Gamma \cos(2\phi_l)$ it uses $\{\Gamma_n\Gamma(\cos(2\phi_l) - (1 - \Gamma_n/\Gamma))\}$, which would readily lead to ENDF-6 expression.

2.2.1 Low energy approximation

In the low energy approximation only s-waves play a role, kR' is small, hence

$$\sin \phi_0 \approx kR' \quad (2.17)$$

and the 3rd term in Eq. (2.16) can be neglected since

$$\Gamma_n^2 \gg 2\Gamma_n\Gamma(kR')^2. \quad (2.18)$$

One thus gets for s-wave neutrons

$$\sigma_n^{pot} \approx 4\pi R'^2 \quad (2.19)$$

and

$$\sigma_n(E) \approx 4\pi R'^2 + \pi\lambda^2 g \frac{\Gamma_n^2 + 2(E - E_0)\Gamma_n \sin(2\phi_0)}{(E - E_0)^2 + \frac{1}{4}\Gamma^2} \quad (2.20)$$

and the area under the elastic scattering resonance, A_n , can be expressed analytically. Since the contribution from the interference term approximately cancels out, the result of integration is similar to the capture kernel and reads [1] (see p.72, Eq.3.3)

$$A_n = \int_{-\infty}^{+\infty} \sigma_n^{res}(E) dE = 2\pi^2 \lambda^2 \frac{g\Gamma_n\Gamma_n}{\Gamma}, \quad (2.21)$$

where the cross section is restricted to the resonance term, $\sigma_n^{res}(E)$. The average scattering cross section in sufficiently broad energy group of the width $\Delta E = E_1 - E_2$ around the resonance energy E_0 can thus be obtained as

$$\bar{\sigma}_n = \frac{1}{\Delta E} \int_{E_2}^{E_1} \sigma_n(E) dE \approx \frac{1}{\Delta E} \int_{E_2}^{E_1} 4\pi R'^2 dE + \frac{1}{\Delta E} \int_{-\infty}^{+\infty} \sigma_n(E) dE, \quad (2.22)$$

which is the sum of potential scattering and resonance scattering,

$$\bar{\sigma}_n = \bar{\sigma}_n^{pot} + \bar{\sigma}_n^{res} \approx 4\pi R'^2 + a \frac{g\Gamma_n\Gamma_n}{\Gamma}, \quad (2.23)$$

with the resonance term being similar to the expression for the average capture cross section.

The low energy approximation should work well up to about 100 keV for lighter nuclei. This can be shown as follows: if the wave number k is expressed in units of cm^{-1} , then the numerical constant in Eq. (2.10) reads 2.197×10^9 . By considering ^{55}Mn with $R' = 4.5$ fm as given in Atlas and $E = 10^5$ eV one gets

$$kR' = 2.197 \times 10^9 \sqrt{E} 4.5 \times 10^{-13} \approx 10^{-3} \sqrt{E} \approx 0.3,$$

meaning that kR' is still sufficiently small so that $\sin(kR') \approx kR'$. For heavy nuclei such as ^{235}U the scattering radius is much larger, $R' = 9.6$ fm, and the energy limit at which $kR' \approx 0.3$ drops to about 20 keV.

It is instructive to compute the average resonance scattering cross section using Eq. (2.23). We consider the 1st resonance of ^{55}Mn at $E_0 = 337$ eV and use ENDF/B-VII.0 parameters [12]: $J = 2$ implying $g = 5/12$, $\Gamma_n = 21.99$ eV, $\Gamma_\gamma = 0.31$ eV, $\Gamma = 22.30$ eV and $R' = 5.15$ fm. Assuming $\Delta E = 500$ eV $\approx 22 \Gamma$ one gets

$$\bar{\sigma}_n^{res} = a \frac{g\Gamma_n^2}{\Gamma} = a \frac{5}{12} \times 21.99 \times \frac{21.99}{22.30} = 9.035 a,$$

with

$$a = 4.089 \times 10^6 \frac{(A+1)^2}{A^2} \frac{1}{E_0 \Delta E} = \frac{4.089 \times (56/55)^2 \times 10^6}{3.37 \times 10^2 \times 5 \times 10^2} = 25.16$$

giving

$$\bar{\sigma}_n^{res} = 25.16 \times 9.035 = 227.3 b.$$

This cross section compares well with the value obtained by Sigma retrieval system [13] applied to ENDF/B-VII.0 and integrated from 150 eV to 650 eV,

$$\bar{\sigma}_n^{res} = 228 b - 3.3 b \approx 225 b,$$

which was corrected for the potential scattering cross section

$$\bar{\sigma}_n^{pot} = 4\pi R'^2 = 4\pi (5.15 \times 10^{-13} \text{ cm})^2 = 3.3 b.$$

Also if one considers a symmetrical cut by $\pm 10\Gamma$ around 337 eV, from 114 eV to 560 eV, one obtains 249 b from the kernel and 251 b from Sigma.

2.2.2 Approximations at higher energies

Eq. (2.23) is applicable in the low-energy approximation which is reasonable for many nuclei of practical interest. For materials such as Cr, Fe and Ni, however, the resonance region extends up to hundreds of keV, *e.g.*, 850 keV for ^{56}Fe . In these cases the low-energy approximation is no more valid above about 100 keV and two effects should be taken into account. First, potential scattering should be directly computed from phase shifts,

$$\sigma_n^{pot}(E) = 4\pi\lambda^2(2l+1)\sin^2\phi_l. \quad (2.24)$$

Second, the full resonance term

$$\Gamma_n^2 - 2\Gamma_n\Gamma\sin^2\phi_l \quad (2.25)$$

should be preserved in Eq. (2.20). Considering that $\sigma_n^{pot}(E)$ is slowly varying function of energy and the dominant contribution to integral of the resonance term comes from relatively narrow energy range (compared to E) around E_0 , where $\sin^2 \phi_l$ can be considered to be approximately constant, one gets

$$\bar{\sigma}_n \approx \sigma_n^{pot}(\bar{E}) + a \frac{g\Gamma_n(\Gamma_n - 2\Gamma \sin^2 \phi_l)}{\Gamma}, \quad (2.26)$$

where $\bar{E} \approx E_0$ and $\sin^2 \phi_l$ is approximated with the value computed at E_0 .

2.2.3 Role of outside resonances

It should be noted that an evaluator of resonance parameters, MF2, would likely introduce resonances outside the resolved resonance energy region (RRR). In computing average cross sections these resonances would be accounted for by processing codes, but not by kernel equations. Therefore, one should be aware of it and be careful when comparing kernel and NJOY results.

- Bound resonances. These are introduced primarily to fix thermal region. However, their elastic scattering tail might extend to much higher energies depending on their neutron width. We note that in some cases they are really large.
- High energy resonances. These are introduced primarily to take care of contribution from missing resonances. Again, if their width is too large, the tails would extend to much lower energies.

Chapter 3

Covariances for a single resonance

In the kernel approximation a single resonance is described its average cross section. Hence, covariance for a single resonance is just one number, uncertainty of the average cross section.

A comment should be made on terminology used throughout this paper. We will use the term **uncertainty** for the quantity known in statistical mathematics as **standard deviation**, which is square root of **variance**.

3.1 Radiative capture

3.1.1 Computation directly from kernels

Capture kernels along with uncertainties are often readily provided in the Atlas of Neutron Resonances. This is the case for many nuclides, including priority materials for reactor applications such as ^{23}Na , ^{27}Al , $^{50,52,53}\text{Cr}$, $^{54,56,57}\text{Fe}$, $^{58,60}\text{Ni}$, ^{90}Zr , some fission products and others. This means that one can retrieve from Atlas all necessary quantities,

$$\frac{g\Gamma_n\Gamma_\gamma}{\Gamma} = \frac{1}{a}A_\gamma \quad (3.1)$$

and

$$\Delta \frac{g\Gamma_n\Gamma_\gamma}{\Gamma} = \frac{1}{a}\Delta A_\gamma, \quad (3.2)$$

needed to compute uncertainty of the average capture cross section. If the evaluator decides to use this handy information, then the computation of the relative

uncertainty of the average capture cross section for a single resonance is straightforward

$$\frac{\Delta\bar{\sigma}_\gamma}{\sigma_\gamma} = \frac{\Delta A_\gamma}{A_\gamma}. \quad (3.3)$$

3.1.2 Computation from resonance parameters

Covariances of average (group) capture cross section can be obtained by folding cross section sensitivities with the covariances of the resonance parameters. For a single resonance one gets

$$\langle\delta\bar{\sigma}_\gamma\delta\bar{\sigma}_\gamma\rangle = \sum_{i,j} \frac{\partial\bar{\sigma}_\gamma}{\partial p_i} \langle\delta p_i\delta p_j\rangle \frac{\partial\bar{\sigma}_\gamma}{\partial p_j}, \quad (3.4)$$

where p_i, p_j are the resonance parameters and $\langle\delta p_i\delta p_j\rangle$ is their covariance. Neglecting contributions from the imperfect knowledge of the resonance energy E_0 and spin J and considering only $i, j = \Gamma_n, \Gamma_\gamma$ one gets

$$\langle\delta\bar{\sigma}_\gamma\delta\bar{\sigma}_\gamma\rangle = \frac{\partial\bar{\sigma}_\gamma}{\partial\Gamma_n} \langle\delta\Gamma_n\delta\Gamma_n\rangle \frac{\partial\bar{\sigma}_\gamma}{\partial\Gamma_n} + 2 \frac{\partial\bar{\sigma}_\gamma}{\partial\Gamma_\gamma} \langle\delta\Gamma_\gamma\delta\Gamma_n\rangle \frac{\partial\bar{\sigma}_\gamma}{\partial\Gamma_n} + \frac{\partial\bar{\sigma}_\gamma}{\partial\Gamma_\gamma} \langle\delta\Gamma_\gamma\delta\Gamma_\gamma\rangle \frac{\partial\bar{\sigma}_\gamma}{\partial\Gamma_\gamma}. \quad (3.5)$$

Sensitivities

We proceed by deriving analytical expressions for sensitivities. These are defined as partial derivatives of the kernel with respect to Γ_n and Γ_γ , and in principle also E_0 and J . Using Eq. (2.8) one gets

$$\frac{\partial\bar{\sigma}_\gamma}{\partial\Gamma_n} = ag \frac{\partial}{\partial\Gamma_n} \frac{\Gamma_n\Gamma_\gamma}{\Gamma} = ag\Gamma_\gamma \left(\frac{1}{\Gamma} - \frac{\Gamma_n}{\Gamma^2} \right) = ag \frac{\Gamma_\gamma^2}{\Gamma^2} \quad (3.6)$$

and

$$\frac{\partial\bar{\sigma}_\gamma}{\partial\Gamma_\gamma} = ag \frac{\partial}{\partial\Gamma_\gamma} \frac{\Gamma_n\Gamma_\gamma}{\Gamma} = ag\Gamma_n \left(\frac{1}{\Gamma} - \frac{\Gamma_\gamma}{\Gamma^2} \right) = ag \frac{\Gamma_n^2}{\Gamma^2}. \quad (3.7)$$

These equations can be re-written to their final form that shows sensitivities in more transparent and useful way

$$\frac{\partial\bar{\sigma}_\gamma}{\partial\Gamma_n} = a \frac{g\Gamma_n\Gamma_\gamma}{\Gamma} \frac{\Gamma_\gamma}{\Gamma} \frac{1}{\Gamma_n} = \bar{\sigma}_\gamma \frac{\Gamma_\gamma}{\Gamma} \frac{1}{\Gamma_n} \quad (3.8)$$

and

$$\frac{\partial \bar{\sigma}_\gamma}{\partial \Gamma_\gamma} = a \frac{g \Gamma_n \Gamma_\gamma}{\Gamma} \frac{\Gamma_n}{\Gamma} \frac{1}{\Gamma_\gamma} = \bar{\sigma}_\gamma \frac{\Gamma_n}{\Gamma} \frac{1}{\Gamma_\gamma}. \quad (3.9)$$

For completeness we also derive partial derivatives with respect to the resonance energy E_0 and spin J . In doing so one should consider just the term g/E_0 in the expression for $\bar{\sigma}_\gamma$

$$\frac{g}{E_0} = \frac{2J+1}{2(2I+1)} \frac{1}{E_0}. \quad (3.10)$$

Partial derivative with respect to E_0 reads

$$\frac{\partial}{\partial E_0} \frac{1}{E_0} = -\frac{1}{E_0^2} = -\frac{1}{E_0} \frac{1}{E_0}, \quad (3.11)$$

implying

$$\frac{\partial \bar{\sigma}_\gamma}{\partial E_0} \approx -\bar{\sigma}_\gamma \frac{1}{E_0}. \quad (3.12)$$

Partial derivative with respect to J should take into account quantum-mechanical nature of spin, minimal change of spin being $\Delta J = \pm 1$. Since g is simple linear function of J one gets

$$\frac{\partial}{\partial J} g = \frac{\partial(2J+1)}{\partial J} \frac{1}{2(2I+1)} = \frac{2\partial J}{\partial J} \frac{1}{2(2I+1)} = \frac{1}{2I+1} \quad (3.13)$$

irrespective whether ∂J is treated as infinitesimally small quantity or as $\Delta J = \pm 1$. Therefore

$$\frac{\partial}{\partial J} g = \frac{2J}{2(2J+1)} \frac{1}{J} \approx g \frac{1}{J} \quad (3.14)$$

and

$$\frac{\partial \bar{\sigma}_\gamma}{\partial J} \approx \bar{\sigma}_\gamma \frac{1}{J}. \quad (3.15)$$

The above sensitivities can be checked against the expressions in PUFF-IV Manual [5]. They are in full agreement except for sensitivity to J , where we included relatively small additive term to preserve convenient compact expression proportional to $\bar{\sigma}_\gamma$.

It should be noted that resonance energies are typically known to $\Delta E_0 \approx 0.1\%$ precision and their contribution to cross section uncertainties in vast majority of cases can be neglected. One should be careful, however, when dealing with those few nuclei where the resonance region starts at very low energies. If E_0 is close to thermal point even small shift in the resonance energy might have strong impact on the thermal cross section and its uncertainty.

Uncertainties caused by the lack of knowledge of resonance spins can be much higher and easily reach 40% or so. As a rule, however, Atlas supplies $g\Gamma_n$ or $2g\Gamma_n$ values rather than Γ_n , reducing thus the need for explicit inclusion of spin in the uncertainty budget. If, however, the ratio Γ_n/Γ or Γ_γ/Γ cannot be well approximated, then explicit knowledge of Γ_n is needed and ΔJ should be taken into account.

Covariances

Using the sensitivities given by $\partial\bar{\sigma}_\gamma/\partial\Gamma_\gamma$ and $\partial\bar{\sigma}_\gamma/\partial\Gamma_n$, the covariance for the average capture cross section can be expressed as

$$\frac{\langle\delta\bar{\sigma}_\gamma\delta\bar{\sigma}_\gamma\rangle}{\bar{\sigma}_\gamma^2} = \left(\frac{\Gamma_\gamma}{\Gamma}\right)^2 \frac{\langle\delta\Gamma_n\delta\Gamma_n\rangle}{\Gamma_n^2} + 2\frac{\Gamma_n\Gamma_\gamma}{\Gamma^2} \frac{\langle\delta\Gamma_n\delta\Gamma_\gamma\rangle}{\Gamma_n\Gamma_\gamma} + \left(\frac{\Gamma_n}{\Gamma}\right)^2 \frac{\langle\delta\Gamma_\gamma\delta\Gamma_\gamma\rangle}{\Gamma_\gamma^2}. \quad (3.16)$$

This equation allows the absolute covariance terms to be readily converted to their relative values so that we finally obtain

$$(\Delta\bar{\sigma}_\gamma)^2 = \left(\frac{\Gamma_\gamma}{\Gamma}\Delta\Gamma_n\right)^2 + 2\frac{\Gamma_n\Gamma_\gamma}{\Gamma^2}\langle\Delta\Gamma_n\Delta\Gamma_\gamma\rangle + \left(\frac{\Gamma_n}{\Gamma}\Delta\Gamma_\gamma\right)^2, \quad (3.17)$$

where $\Delta\sigma_\gamma$, $\Delta\Gamma_n$ and $\Delta\Gamma_\gamma$ are relative uncertainties and $\langle\Delta\Gamma_n\Delta\Gamma_\gamma\rangle$ denotes relative correlation between the neutron width and radiative width.

Eq. (3.17) represents our concluding expression for a single resonance. It shows how the uncertainty of the average (group) capture cross section should be computed. One can easily see that if Γ_n is much larger than Γ_γ , then both the 1st and 2nd term can be neglected and

$$\Delta\bar{\sigma}_\gamma \approx \frac{\Gamma_n}{\Gamma}\Delta\Gamma_\gamma \approx \Delta\Gamma_\gamma \text{ if } \Gamma_n \gg \Gamma_\gamma. \quad (3.18)$$

This situation occurs for many strong resonances which in general are s-wave resonances, an example would be ^{55}Mn .

Eq. (3.17) also shows that, unless neutron and radiative width are comparable, the 2nd term can be neglected even if the correlation between neutron and radiative widths would be strong. This in practice means that $\Gamma_n \propto \Gamma_\gamma$ correlation for a single resonance makes little or no impact on the average capture cross section uncertainty.

We proceed with the application of the above formalism to ^{55}Mn capture by examining the first 6 strong resonances, with resonance strength defined by the capture kernel, see Table 3.1. The target spin is $I = 5/2$, implying $2g = 5/6 = 0.83$ for resonances with spin $J = 2$ and $2g = 7/6 = 1.17$ for $J = 3$. We note that ^{55}Mn is almost pure scatterer, meaning that $\Gamma_n \gg \Gamma_\gamma$, hence $\Delta\Gamma_\gamma = \delta\Gamma_\gamma/\Gamma_\gamma$ defines the average capture cross section uncertainty $\Delta\bar{\sigma}_\gamma$. A comparison is made with the uncertainties given in AFCE-1.2 library [14]. This library is produced in 33-energy group representation, mostly with groups of the same lethargy 0.5, starting in reverse order with group 1 (19.6 MeV - 10 MeV), down through group 22 (454 eV - 304 eV) to group 33 (10^{-1} eV - 10^{-5} eV).

Table 3.1: Example of $^{55}\text{Mn}(n,\gamma)$ resonances. Shown are first 6 strong capture resonances determined by the value of capture kernel, A_γ .

E_0 keV	J	l	$2g\Gamma_n$ eV	$\delta 2g\Gamma_n$ eV	Γ_γ eV	$\delta\Gamma_\gamma$ eV	A_γ/a	$\Delta\bar{\sigma}_\gamma$ %	AFCE %
0.337	2	0	18.3	0.4	0.31	0.02	0.13	6.4	5.2
1.09	2	0	18	0.8	0.435	0.1	0.18	22.5	21
2.32	3	0	460	24	0.34	0.13	0.20	38.2	23
4.90		1	0.932		0.29	0.013	0.11	3.4	4.1
7.10	2	0	332	8	1.03	0.08	0.43	7.7	
8.80	3	0	432	12	0.82	0.08	0.48	9.7	5.0 ^a

^a Refers to uncertainty in group no.16 with two resonances, $E_0 = 7.10, 8.80$ keV.

A comment should be made on the p-wave resonance at 4.9 keV with unknown spin J. Related uncertainty ΔJ is partly taken care of by the combined

quantity $2g\Gamma_n$. Spin uncertainty cannot, however, be fully neglected, it contributes to Γ , where Γ_n rather than $2g\Gamma_n$ steps in. The value $\Delta\bar{\sigma}_\gamma = 3.4\%$ in Table 3.1 does not account for this contribution and it is thus somewhat underestimated.

3.2 Elastic scattering

According to Eq. (2.23) the average elastic scattering cross section has two terms, the resonance scattering and potential scattering. Therefore, elastic scattering covariances should be obtained by quadratic summation of these two contributions,

$$(\Delta\bar{\sigma}_n)^2 = \left(\frac{\bar{\sigma}_n^{res}}{\bar{\sigma}_n} \Delta\bar{\sigma}_n^{res} \right)^2 + 2 \frac{\bar{\sigma}_n^{res}}{\bar{\sigma}_n} \langle \Delta\bar{\sigma}_n^{res} \Delta\bar{\sigma}_n^{pot} \rangle \frac{\bar{\sigma}_n^{pot}}{\bar{\sigma}_n} + \left(\frac{\bar{\sigma}_n^{pot}}{\bar{\sigma}_n} \Delta\bar{\sigma}_n^{pot} \right)^2. \quad (3.19)$$

This expression is general and includes also the term due to possible correlation between potential and resonance scattering. What remains to be derived are expressions for relative uncertainties $\Delta\bar{\sigma}_n^{res}$, $\Delta\bar{\sigma}_n^{pot}$.

3.2.1 Resonance contribution

Similarly to capture we derive sensitivities of the average elastic resonance scattering cross section $\bar{\sigma}_n^{res}$ with respect to the resonance parameters.

Low energy approximation

Starting from Eq. (2.23) one gets

$$\frac{\partial\bar{\sigma}_n^{res}}{\partial\Gamma_n} = ag \frac{\partial}{\partial\Gamma_n} \frac{\Gamma_n^2}{\Gamma} = ag \left(\frac{2\Gamma_n}{\Gamma} - \frac{\Gamma_n^2}{\Gamma^2} \right) = ag \frac{\Gamma_n}{\Gamma} \frac{\Gamma + \Gamma_\gamma}{\Gamma} \quad (3.20)$$

and

$$\frac{\partial\bar{\sigma}_n^{res}}{\partial\Gamma_\gamma} = ag \frac{\partial}{\partial\Gamma_\gamma} \frac{\Gamma_n^2}{\Gamma} = ag\Gamma_n^2 \frac{\partial}{\partial\Gamma_\gamma} \frac{1}{\Gamma} = -ag \frac{\Gamma_n^2}{\Gamma^2}. \quad (3.21)$$

Using Eq. (2.23) these relations can be transformed into expressions more suitable for our purposes

$$\frac{\partial\bar{\sigma}_n^{res}}{\partial\Gamma_n} = ag \frac{\Gamma_n^2}{\Gamma} \frac{\Gamma + \Gamma_\gamma}{\Gamma\Gamma_n} = \bar{\sigma}_n^{res} \frac{\Gamma + \Gamma_\gamma}{\Gamma} \frac{1}{\Gamma_n} \quad (3.22)$$

and

$$\frac{\partial \bar{\sigma}_n^{res}}{\partial \Gamma_\gamma} = -ag \frac{\Gamma_n^2}{\Gamma} \frac{1}{\Gamma} = -\bar{\sigma}_n^{res} \frac{\Gamma_\gamma}{\Gamma} \frac{1}{\Gamma_\gamma}. \quad (3.23)$$

Using the above expressions for sensitivities the covariance for the average resonance scattering cross section can be expressed as

$$\frac{\langle \delta \bar{\sigma}_n^{res} \delta \bar{\sigma}_n^{res} \rangle}{(\bar{\sigma}_n^{res})^2} = \left(\frac{\Gamma + \Gamma_\gamma}{\Gamma} \right)^2 \frac{\langle \delta \Gamma_n \delta \Gamma_n \rangle}{\Gamma_n^2} - 2 \frac{\Gamma + \Gamma_\gamma}{\Gamma} \frac{\Gamma_\gamma}{\Gamma} \frac{\langle \delta \Gamma_n \delta \Gamma_\gamma \rangle}{\Gamma_n \Gamma_\gamma} + \left(\frac{\Gamma_\gamma}{\Gamma} \right)^2 \frac{\langle \delta \Gamma_\gamma \delta \Gamma_\gamma \rangle}{\Gamma_\gamma^2}. \quad (3.24)$$

The absolute covariances can be readily replaced by their relative values so that we finally obtain

$$(\Delta \bar{\sigma}_n^{res})^2 = \left(\frac{\Gamma + \Gamma_\gamma}{\Gamma} \Delta \Gamma_n \right)^2 - 2 \frac{(\Gamma + \Gamma_\gamma) \Gamma_\gamma}{\Gamma^2} \langle \Delta \Gamma_n \Delta \Gamma_\gamma \rangle + \left(\frac{\Gamma_\gamma}{\Gamma} \Delta \Gamma_\gamma \right)^2. \quad (3.25)$$

What apparently counts in many cases in practice is the first term of Eq. (3.25) only. One can readily see that if Γ_n is much larger than Γ_γ , then both multiplicative and additive terms containing Γ_γ can be neglected and the average elastic resonance scattering cross section uncertainty is

$$\Delta \bar{\sigma}_n^{res} \approx \Delta \Gamma_n \text{ if } \Gamma_n \gg \Gamma_\gamma. \quad (3.26)$$

This holds for many strong elastic scattering resonances, such as essentially all s-wave resonances in ^{55}Mn . It should be noted, however, that other scenarios take place, such as $\Gamma_n < \Gamma_\gamma$ for fission products at low energies, for which the 3rd term contributes and cannot be neglected.

The other limiting case occurs when Γ_n is much smaller than Γ_γ , implying $\Gamma \approx \Gamma_\gamma$. The uncertainty of the group cross section becomes

$$\Delta \bar{\sigma}_n^{res} \approx \sqrt{(2\Delta \Gamma_n)^2 + (\Delta \Gamma_\gamma)^2} \text{ if } \Gamma_n \ll \Gamma_\gamma, \quad (3.27)$$

assuming that correlation between Γ_n and Γ_γ is small. This limiting case, however, implies that the scattering kernel is very small as well. Hence, the average scattering cross section is small and the resonance does not contribute much to elastic processes. This suggests that potential scattering and thus $\Delta R'$ (if known)

Table 3.2: Example of $^{55}\text{Mn}(n,\text{el})$ resonances. Shown are first 6 strong resonances determined by the value of the scattering kernel, A_n . The last two resonances fall into one group in AFCI-1.2 covariance library [14].

E_0 keV	J	l	$2g\Gamma_n$ eV	$\delta 2g\Gamma_n$ eV	Γ_γ eV	$\delta\Gamma_\gamma$ eV	A_n/a	$\Delta\bar{\sigma}_n^{res}$ %	AFCI %	Group No.
0.337	2	0	18.3	0.4	0.31	0.02	10.8	2.2	5.0	22
1.09	2	0	18	0.8	0.435	0.1	10.6	4.4	3.9	20
2.32	3	0	460	24	0.34	0.13	197	5.2	2.4	18
4.90		1	0.932		0.29	0.013	0.4		5.2	17
7.10	2	0	332	8	1.03	0.08	199	2.4		16
8.80	3	0	432	12	0.82	0.08	185	2.8	1.4 ^a	16

^a Refers to uncertainty in group no.16 with two resonances, $E_0 = 7.10, 8.80$ keV.

represents more important component in the corresponding energy range.

As an example in Table 3.2 we show 6 first strong elastic scattering resonances in ^{55}Mn . One can see that s-wave resonances are very strong and the only p-wave resonance in this short list is weak and does not contribute significantly to overall uncertainty budget.

Approximation suitable for higher energies

At higher energies the low energy approximation is no more valid and one has to resort to full expressions. In practice this means to use

$$\bar{\sigma}_n^{res} = a \frac{g\Gamma_n\Gamma_n}{\Gamma} - 2ag\Gamma_n \sin^2 \phi_l. \quad (3.28)$$

As a consequence the sensitivity with respect to Γ_n , Eq. (3.20), has one more term and reads

$$\frac{\partial \bar{\sigma}_n^{res}}{\partial \Gamma_n} = ag \frac{\Gamma_n}{\Gamma} \frac{\Gamma + \Gamma_\gamma}{\Gamma} - 2ag \sin^2 \phi_l, \quad (3.29)$$

meaning that it is reduced compared to the low energy approximation and eventually it may reach zero. On the other hand, the sensitivity with respect to Γ_γ , Eq. (3.21), remains the same. In addition, however, we have also sensitivity with

respect to R' ,

$$\frac{\partial \bar{\sigma}_n^{res}}{\partial R'} = 4akg\Gamma_n \sin \phi_l \cos \phi_l. \quad (3.30)$$

3.2.2 Potential scattering contribution

In the low energy approximation the contribution to elastic scattering covariances from potential scattering can be readily obtained from Eq. (2.19). One computes sensitivity

$$\frac{\partial \sigma_n^{pot}}{\partial R'} = \frac{\partial(4\pi R'^2)}{\partial R'} = 8\pi R' \quad (3.31)$$

and obtains relative uncertainty of the potential scattering cross section as

$$\Delta \sigma_n^{pot} = \frac{\partial \sigma_n^{pot}}{\partial R'} \frac{\delta R'}{\sigma_n^{pot}} = \frac{8\pi R'}{4\pi R'^2} \delta R' = 2 \frac{\delta R'}{R'} = 2\Delta R'. \quad (3.32)$$

At high energies one should resort to full expression for the potential scattering. By summing up s- and p-waves and neglecting d-waves as well as distant level contributions, Eq. (2.24) gives

$$\sigma_n^{pot}(E) = \frac{4\pi}{k^2} \left\{ \sin^2 kR' + 3 \sin^2(kR' - \arctan kR') \right\} \quad (3.33)$$

or

$$\sigma_n^{pot}(E) = \frac{4\pi}{k^2} \left\{ \sin^2 \phi_0 + 3 \sin^2 \phi_1 \right\}. \quad (3.34)$$

The sensitivity is given as

$$\frac{\partial \sigma_n^{pot}}{\partial R'} = \frac{4\pi}{k^2} \left\{ \frac{\partial \sin^2 \phi_0}{\partial R'} + 3 \frac{\partial \sin^2 \phi_1}{\partial R'} \right\}, \quad (3.35)$$

where the derivative of the s-wave term is

$$\frac{\partial \sin^2 \phi_0}{\partial R'} = 2 \sin \phi_0 \cos \phi_0 \frac{\partial \phi_0}{\partial R'} = 2k \sin \phi_0 \cos \phi_0 \quad (3.36)$$

and that of the p-wave reads

$$\frac{\partial \sin^2 \phi_1}{\partial R'} = 2 \sin \phi_1 \cos \phi_1 \frac{\partial \phi_1}{\partial R'},$$

$$\frac{\partial \phi_1}{\partial R'} = \frac{\partial(kR' - \arctan kR')}{\partial R'} = k \left\{ 1 - \frac{1}{1 + (kR')^2} \right\}. \quad (3.37)$$

By putting these partial results together one gets

$$\frac{\partial \sigma_n^{pot}}{\partial R'} = \frac{8\pi}{k} \left\{ \sin \phi_0 \cos \phi_0 + 3 \left(1 - \frac{1}{1 + (kR')^2} \right) \sin \phi_1 \cos \phi_1 \right\}, \quad (3.38)$$

which reduces to Eq. (3.31) at low energies as expected.

Then, the relative uncertainty of full potential scattering

$$\Delta \sigma_n^{pot} = \frac{\partial \sigma_n^{pot}}{\partial R'} \frac{\delta R'}{\sigma_n^{pot}}$$

can be expressed as

$$\Delta \sigma_n^{pot} = 2\Delta R' \left\{ kR' \frac{\sin \phi_0 \cos \phi_0 + 3 \left(1 - \frac{1}{1 + (kR')^2} \right) \sin \phi_1 \cos \phi_1}{\sin^2 \phi_0 + 3 \sin^2 \phi_1} \right\}, \quad (3.39)$$

which reduces to Eq. (3.32) at low energies. The term in large brackets can be viewed as the uncertainty correction to the low energy approximation. For illustration we show in Table 3.3 this correction for ^{56}Fe . As can be seen the deviation from unity is fairly small even at 800 keV which is close to the upper end of the resolved resonance region of ^{56}Fe .

Table 3.3: Correction term for the relative uncertainty of the potential scattering cross section for ^{56}Fe . Value of $R' = 5.9$ fm was assumed (Atlas).

Energy keV	ϕ_0 radian	ϕ_1 radian	s-wave barn	p-wave barn	σ_n^{pot} barn	Uncertainty correction
10	0.127	0.001	4.35	0.00	4.35	0.995
100	0.403	0.020	4.14	0.03	4.17	0.960
200	0.569	0.052	3.92	0.11	4.03	0.938
500	0.784	0.167	3.31	0.45	3.76	0.914
800	1.139	0.289	2.78	0.82	3.60	0.898

Chapter 4

Covariances for many resonances

The previous analysis for a single isolated resonance can be extended to many resonances located in one energy group. We proceed step by step so that all details of the procedure can be clearly followed. The formalism described below is applicable both to capture and scattering, hence whenever appropriate, we use notation $\bar{\sigma}$ and drop the subscripts γ and n .

4.1 Formalism for many resonances

The average cross section due to several resonances located in one energy group can be obtained as

$$\bar{\sigma} = \frac{1}{\Delta E} \int_{E_2}^{E_1} \sum_r \sigma_r(E) dE = \sum_r \bar{\sigma}_r, \quad (4.1)$$

where the summation goes over all resonances r in the energy interval ΔE . It should be noted that this equation represents good approximation of capture (and fission), but it is less suitable for elastic scattering, for which multilevel Breit-Wigner or Reich-Moore formalism should be adopted. This means that coherent summation of scattering amplitudes should be applied rather than their incoherent summation assumed by Eq. (4.1). Despite this, the proposed approach should represent sufficiently plausible approximation of elastic cross sections averaged over broader energy groups.

The sensitivities can be computed as partial derivatives of $\bar{\sigma}$ with respect to resonance parameters $p_{i,r}$ where $i = \gamma, n$. Thus,

$$\frac{\partial \bar{\sigma}}{\partial p_{i,r}} = \sum_{r'} \frac{\partial \bar{\sigma}_{r'}}{\partial p_{i,r}} = \frac{\partial \bar{\sigma}_r}{\partial p_{i,r}}, \quad (4.2)$$

meaning that the sensitivity for only one resonance remains on the right hand side, since each resonance is defined by its own set of resonance parameters and does not depend on the parameters of other resonances.

Using these sensitivities the covariance of the group cross section $\bar{\sigma}$ can be obtained as

$$\langle \delta \bar{\sigma} \delta \bar{\sigma} \rangle = \sum_{i,r,i',r'} \frac{\partial \bar{\sigma}}{\partial p_{i,r}} \langle \delta p_{i,r} \delta p_{i',r'} \rangle \frac{\partial \bar{\sigma}}{\partial p_{i',r'}}, \quad (4.3)$$

where $\langle \delta p_{i,r} \delta p_{i',r'} \rangle$ is the covariance of resonance parameters.

By dividing Eq (4.3) with the average cross section one gets expression for the relative covariance

$$\frac{\langle \delta \bar{\sigma} \delta \bar{\sigma} \rangle}{\bar{\sigma}^2} = \sum_{i,r,i',r'} \frac{1}{\bar{\sigma}} \frac{\partial \bar{\sigma}_r}{\partial p_{i,r}} \langle \delta p_{i,r} \delta p_{i',r'} \rangle \frac{1}{\bar{\sigma}} \frac{\partial \bar{\sigma}_{r'}}{\partial p_{i',r'}}. \quad (4.4)$$

Using explicit expressions for the sensitivities derived in the previous Chapter and making appropriate assumptions about the correlations between the resonance parameter uncertainties one can get the uncertainty of the group cross section.

4.2 Explicit treatment of two resonances

To clarify the above formalism we explicitly show its implementation for two resonances located in one energy group.

4.2.1 Capture computed directly from kernels

If one already knows uncertainties of capture kernels, then the procedure for computing uncertainty of the group cross section is fairly straightforward. The group kernel,

$$A_\gamma = A_{\gamma 1} + A_{\gamma 2}, \quad (4.5)$$

has absolute uncertainty

$$(\delta A_\gamma)^2 = (\delta A_{\gamma 1})^2 + 2 \langle \delta A_{\gamma 1} \delta A_{\gamma 2} \rangle + (\delta A_{\gamma 2})^2 \quad (4.6)$$

implying relative uncertainty

$$\left(\frac{\delta A_\gamma}{A_\gamma} \right)^2 = \left(\frac{A_{\gamma 1} \delta A_{\gamma 1}}{A_\gamma A_{\gamma 1}} \right)^2 + 2 \frac{A_{\gamma 1}}{A_\gamma} \left\langle \frac{\delta A_{\gamma 1}}{A_{\gamma 1}} \frac{\delta A_{\gamma 2}}{A_{\gamma 2}} \right\rangle \frac{A_{\gamma 2}}{A_\gamma} + \left(\frac{A_{\gamma 2} \delta A_{\gamma 2}}{A_\gamma A_{\gamma 2}} \right)^2$$

and meaning that

$$(\Delta A_\gamma)^2 = \left(\frac{A_{\gamma 1}}{A_\gamma} \Delta A_{\gamma 1} \right)^2 + 2 \frac{A_{\gamma 1}}{A_\gamma} \langle \Delta A_{\gamma 1} \Delta A_{\gamma 2} \rangle \frac{A_{\gamma 2}}{A_\gamma} + \left(\frac{A_{\gamma 2}}{A_\gamma} \Delta A_{\gamma 2} \right)^2. \quad (4.7)$$

Assuming maximum correlation between the two resonances

$$\langle \Delta A_{\gamma 1} \Delta A_{\gamma 2} \rangle = \Delta A_{\gamma 1} \Delta A_{\gamma 2} \quad (4.8)$$

implies that the group cross section uncertainty is given by simple linear weighted average of the two components,

$$(\Delta A_\gamma)^2 = \left(\frac{A_{\gamma 1}}{A_\gamma} \Delta A_{\gamma 1} + \frac{A_{\gamma 2}}{A_\gamma} \Delta A_{\gamma 2} \right)^2 \quad (4.9)$$

and thus the group cross section uncertainty is

$$\Delta \bar{\sigma}_\gamma = \Delta A_\gamma = \frac{A_{\gamma 1}}{A_\gamma} \Delta A_{\gamma 1} + \frac{A_{\gamma 2}}{A_\gamma} \Delta A_{\gamma 2} \quad (4.10)$$

as one would intuitively expect.

4.2.2 Capture computed from resonance parameters

We explicitly examine capture with two resonances in one energy group. Eq. (4.3) can be rearranged as

$$\langle \delta \bar{\sigma}_\gamma \delta \bar{\sigma}_\gamma \rangle = \langle \delta \bar{\sigma}_{\gamma 1} \delta \bar{\sigma}_{\gamma 1} \rangle + 2 \langle \delta \bar{\sigma}_{\gamma 1} \delta \bar{\sigma}_{\gamma 2} \rangle + \langle \delta \bar{\sigma}_{\gamma 2} \delta \bar{\sigma}_{\gamma 2} \rangle, \quad (4.11)$$

where the first and the last term are contributions from single resonances, and the 2nd term arises from resonance-resonance correlations. Sensitivities to the parameters of the 1st resonance can be expressed as

$$\frac{\partial \bar{\sigma}_\gamma}{\partial \Gamma_{n1}} = \frac{\partial \bar{\sigma}_{\gamma 1}}{\partial \Gamma_{n1}} = \bar{\sigma}_{\gamma 1} \frac{\Gamma_{\gamma 1}}{\Gamma_1} \frac{1}{\Gamma_{n1}}, \quad (4.12)$$

$$\frac{\partial \bar{\sigma}_\gamma}{\partial \Gamma_{\gamma 1}} = \frac{\partial \bar{\sigma}_{\gamma 1}}{\partial \Gamma_{\gamma 1}} = \bar{\sigma}_{\gamma 1} \frac{\Gamma_{n1}}{\Gamma_1} \frac{1}{\Gamma_{\gamma 1}} \quad (4.13)$$

and similarly for the sensitivities to parameters of the 2nd resonance. Therefore,

$$\langle \delta \bar{\sigma}_{\gamma 1} \delta \bar{\sigma}_{\gamma 1} \rangle = (\bar{\sigma}_{\gamma 1})^2 \left\{ \left(\frac{\Gamma_{\gamma 1}}{\Gamma_1} \frac{\delta \Gamma_{n1}}{\Gamma_{n1}} \right)^2 + 2 \frac{\Gamma_{\gamma 1}}{\Gamma_1} \frac{\Gamma_{n1}}{\Gamma_1} \left\langle \frac{\delta \Gamma_{n1}}{\Gamma_{n1}} \frac{\delta \Gamma_{\gamma 1}}{\Gamma_{\gamma 1}} \right\rangle + \left(\frac{\Gamma_{n1}}{\Gamma_1} \frac{\delta \Gamma_{\gamma 1}}{\Gamma_{\gamma 1}} \right)^2 \right\}$$

and

$$\langle \delta \bar{\sigma}_{\gamma 2} \delta \bar{\sigma}_{\gamma 2} \rangle = (\bar{\sigma}_{\gamma 2})^2 (\dots + \dots + \dots),$$

$$\langle \delta \bar{\sigma}_{\gamma 1} \delta \bar{\sigma}_{\gamma 2} \rangle = \bar{\sigma}_{\gamma 1} \bar{\sigma}_{\gamma 2} (\dots + \dots + \dots + \dots). \quad (4.14)$$

These equations indicate that altogether we have 10 terms which account for all possible combinations of the correlations between the resonance parameters under consideration. Dividing by $\bar{\sigma}_\gamma^2$ we transform the above expressions into relative covariances

$$\frac{\langle \delta \bar{\sigma}_{\gamma 1} \delta \bar{\sigma}_{\gamma 1} \rangle}{\bar{\sigma}_\gamma^2} = \left(\frac{\bar{\sigma}_{\gamma 1}}{\bar{\sigma}_\gamma} \right)^2 \left\{ \left(\frac{\Gamma_{\gamma 1}}{\Gamma_1} \Delta \Gamma_{n1} \right)^2 + 2 \frac{\Gamma_{\gamma 1}}{\Gamma_1} \langle \Delta \Gamma_{n1} \Delta \Gamma_{\gamma 1} \rangle \frac{\Gamma_{n1}}{\Gamma_1} + \left(\frac{\Gamma_{n1}}{\Gamma_1} \Delta \Gamma_{\gamma 1} \right)^2 \right\}$$

and similarly for the other terms

$$\begin{aligned} \frac{\langle \delta \bar{\sigma}_{\gamma 2} \delta \bar{\sigma}_{\gamma 2} \rangle}{\bar{\sigma}_\gamma^2} &= \left(\frac{\bar{\sigma}_{\gamma 2}}{\bar{\sigma}_\gamma} \right)^2 (\dots + \dots + \dots), \\ \frac{\langle \delta \bar{\sigma}_{\gamma 1} \delta \bar{\sigma}_{\gamma 2} \rangle}{\bar{\sigma}_\gamma^2} &= \frac{\bar{\sigma}_{\gamma 1} \bar{\sigma}_{\gamma 2}}{\bar{\sigma}_\gamma^2} (\dots + \dots + \dots + \dots). \end{aligned} \quad (4.15)$$

If $\Gamma_n \gg \Gamma_\gamma$ for both resonances as is the case for ^{55}Mn , then the uncertainty of the capture group cross section is

$$(\Delta \bar{\sigma}_\gamma)^2 = \left(\frac{\bar{\sigma}_{\gamma 1}}{\bar{\sigma}_\gamma} \Delta \Gamma_{\gamma 1} \right)^2 + 2 \frac{\bar{\sigma}_{\gamma 1}}{\bar{\sigma}_\gamma} \langle \Delta \Gamma_{\gamma 1} \Delta \Gamma_{\gamma 2} \rangle \frac{\bar{\sigma}_{\gamma 2}}{\bar{\sigma}_\gamma} + \left(\frac{\bar{\sigma}_{\gamma 2}}{\bar{\sigma}_\gamma} \Delta \Gamma_{\gamma 2} \right)^2. \quad (4.16)$$

This result is expressed as a weighted sum, with the weighting factors given by the relative strength of each resonance. If we further assume that the relative correlation has its maximum value

$$\langle \Delta \Gamma_{\gamma 1} \Delta \Gamma_{\gamma 2} \rangle = \Delta \Gamma_{\gamma 1} \Delta \Gamma_{\gamma 2}, \quad (4.17)$$

then the outcome can be mathematically expressed as a simple weighted average of the two resonance contributions

$$(\Delta\bar{\sigma}_\gamma)^2 = \left(\frac{\bar{\sigma}_{\gamma 1}}{\bar{\sigma}_\gamma} \Delta\Gamma_{\gamma 1} + \frac{\bar{\sigma}_{\gamma 2}}{\bar{\sigma}_\gamma} \Delta\Gamma_{\gamma 2} \right)^2. \quad (4.18)$$

As an example we consider ^{55}Mn and two resonances, $E_0 = 7.10$ keV and 8.80 keV, in one group. After proper weighing which takes into account also E_0 dependence of kernels one gets

$$\Delta\bar{\sigma}_\gamma = \frac{0.43b}{0.91b} 7.7\% + \frac{0.48b}{0.95b} 9.7\% = 8.6\%.$$

4.2.3 Elastic scattering

By repeating the exercise for $\Delta\bar{\sigma}_n^{res}$ under the same condition as above, $\Gamma_n \gg \Gamma_\gamma$, one gets

$$(\Delta\bar{\sigma}_n^{res})^2 = \left(\frac{\bar{\sigma}_{n1}^{res}}{\bar{\sigma}_n^{res}} \Delta\Gamma_{n1} \right)^2 + 2 \frac{\bar{\sigma}_{n1}^{res}}{\bar{\sigma}_n^{res}} \langle \Delta\Gamma_{n1} \Delta\Gamma_{n2} \rangle \frac{\bar{\sigma}_{n2}^{res}}{\bar{\sigma}_n^{res}} + \left(\frac{\bar{\sigma}_{n2}^{res}}{\bar{\sigma}_n^{res}} \Delta\Gamma_{n2} \right)^2. \quad (4.19)$$

As an example, considering again ^{55}Mn resonances at $E_0 = 7.1$ keV and 8.8 keV, with the maximum value of the correlation term,

$$\langle \Delta\Gamma_{n1} \Delta\Gamma_{n2} \rangle = \Delta\Gamma_{n1} \Delta\Gamma_{n2}, \quad (4.20)$$

one can compute uncertainty of the group elastic scattering cross section as simple linear weighted sum

$$\Delta\bar{\sigma}_n^{res} = \frac{\bar{\sigma}_{n1}^{res}}{\bar{\sigma}_n^{res}} \Delta\Gamma_{n1} + \frac{\bar{\sigma}_{n2}^{res}}{\bar{\sigma}_n^{res}} \Delta\Gamma_{n2}. \quad (4.21)$$

yielding

$$\Delta\bar{\sigma}_n = \frac{199b}{384b} 2.4\% + \frac{185b}{384b} 2.8\% = 2.6\%.$$

This is much higher than the 1.4% claimed by AFCI-1.2, where apparently the desired maximum value of the correlation term was not properly accounted for.

The contribution from potential scattering should be added exactly in the same way as done for a single resonance. Thus, $\Delta\sigma_n^{pot}$ should be computed according to Eq.(3.39) and then incorporated into $\Delta\sigma_n$ using Eq.(3.19).

Chapter 5

Covariances in thermal energy range

So far we discussed formalism for estimating covariances in the resonance energy range. For the sake of completeness we will describe also the thermal energy range, where simple, yet fairly reasonable covariance estimates can be made using the approach proposed by M. Williams in 2004 [15].

5.1 Thermal radiative capture

With a few exceptions, such as ^{113}Cd , ^{149}Sm and ^{155}Gd , capture cross sections at low neutron energies follow the well-known $1/v$ law. Westcott factors, ideally equal to unity, are usually used as a measure of the validity of this law. In Table 5.1 we summarize Westcott factors for some of the AFCI priority materials, all of which follow $1/v$ extremely well.

The upper energy limit for applicability of this law is usually considered to be $E_{max} = 10$ eV. In practice it might be higher and closer to the 1st resonance, probably as high as $E_{max} \approx E_{01} - 10 \Gamma_1$, giving about 100 eV for ^{55}Mn ($E_{01} = 337$ eV, $\Gamma_1 = 22.3$ eV). In this energy range

$$\sigma_{\gamma}(E) \approx \sigma_{\gamma}(E_{th}) \sqrt{\frac{E_{th}}{E}}, \quad (5.1)$$

where $E_{th} = 0.0253$ eV is the thermal energy.

Table 5.1: Westcott factors g_w for selected materials based on data in JEFF-3.0 library [16].

Material	g_w	Material	g_w
^{23}Na	1.00008	^{54}Fe	1.00008
^{50}Cr	1.00006	^{56}Fe	1.00007
^{52}Cr	1.00008	^{57}Fe	1.00112
^{53}Cr	1.00007	^{58}Ni	1.00008
^{55}Mn	1.00011	^{60}Ni	1.00004

There is only one degree of freedom, $\sigma_\gamma(E_{th})$, which determines capture cross sections in the entire thermal energy range. Consequently, uncertainties can be estimated as

$$\Delta\sigma_\gamma(E) \approx \Delta\sigma_\gamma(E_{th}), \quad (5.2)$$

and the correlation matrix should reflect 100% energy-energy correlations.

This approach was successfully adopted by the recently completed low-fidelity covariance project [17]. The method is based on well established physics of thermal capture and experimentally determined uncertainties, making it likely the best approach one can use. Application to average capture cross sections is straightforward and is not given here.

5.2 Thermal elastic scattering

5.2.1 Thermal scattering cross section uncertainty

Elastic scattering is of particular importance for moderator materials due to their role in the neutron slowing down process and also for structural materials, such as Cr, Fe and Ni, which are almost pure scatterers. Elastic scattering cross sections are nearly constant over a large portion of thermal energy range. At sub-thermal energies, under the free-gas approximation, this constant behavior changes to $1/v$ due to molecular motion of target nuclei. Thus, at energies defined approximately as $10^{-3} \text{ eV} < E < 10 \text{ eV}$ one has

$$\sigma_n(E) \approx \sigma_n(E_{th}), \quad (5.3)$$

to be replaced by approximately $1/v$ behavior at energies below about 10^{-3} eV which holds for temperatures > 300 K.

In accordance with M. Williams [15] this feature can be utilized for estimating elastic scattering cross section uncertainties. Similar to radiative capture, there is only one degree of freedom, $\sigma_n(E_{th})$, which determines cross sections over the entire thermal energy range. Therefore, relative scattering cross section uncertainty in the thermal region can be approximated as

$$\Delta\sigma_n(E) \approx \Delta\sigma_n(E_{th}) = \Delta\sigma_s, \quad (5.4)$$

where σ_s is the free thermal scattering cross section, which together with its uncertainty can be found in Atlas of Neutron Resonances. Again, the related correlation matrix should be simple and should reflect 100% energy-energy correlations.

5.2.2 Impact of scattering radius uncertainty

A comment should be made on recent attempts to account for scattering radius uncertainty $\Delta R'$ in the uncertainty budget of elastic scattering. On the first glance this is a correct idea, which, however, should be applied with caution. The point is that the scattering radius is a derived quantity which in most cases has much higher uncertainty than σ_s which is measured directly.

To make our point we show how $\Delta R'$ and $\Delta\sigma_s$ are coupled, using expressions derived in Atlas on pp. 4-5. The thermal scattering cross section is given by the sum of coherent and incoherent terms,

$$\sigma_s = \sigma_{coh} + \sigma_{incoh}, \quad (5.5)$$

where

$$\sigma_{coh} = 4\pi a^2, \quad (5.6)$$

the scattering coherent length being

$$a \approx R' - 2.277 \times 10^3 \frac{A+1}{A} \sum_j \frac{g\Gamma_{nj}^0}{E_j} = R' - b. \quad (5.7)$$

Here, Γ_{nj}^0 is the reduced neutron width and summation goes over all resonances (positive and bound). We note that a might be a negative quantity. Eq. (5.7) was

used in many cases to obtain $\Delta R'$ in Atlas,

$$(\Delta R')^2 \approx (\Delta a)^2 + 2.277 \times 10^3 \frac{A+1}{A} \sum_j \left(\frac{\Delta g \Gamma_{nj}^0}{E_j} \right)^2. \quad (5.8)$$

Usually Δa is small, hence $\Delta \Gamma_{nj}^0$ determines $\Delta R'$ meaning that these quantities are strongly correlated. Eq. (5.8) also shows how the scattering radius uncertainty impacts $\Delta \sigma_{coh}$ and thus also $\Delta \sigma_s$.

The trouble starts when one attempts to compute impact of $\Delta R'$ on $\Delta \sigma_s$ using usual propagation of errors for uncorrelated quantities. Computing the sensitivity for the coherent scattering term as

$$\frac{\partial \sigma_{coh}}{\partial R'} = 8\pi a \frac{\partial a}{\partial R'} = 8\pi(R' - b) \quad (5.9)$$

one gets the absolute uncertainty

$$\delta \sigma_{coh} = 8\pi |R' - b| \delta R'. \quad (5.10)$$

In the case of ^{55}Mn $\sigma_s = 2.06$ b is mostly due to coherent scattering, $\sigma_{coh} = 1.734$ b, the coherent scattering length being negative. Therefore, $R' = 4.5$ fm requires $b = 8.22$ fm to get 1.734 b. Using Eq. (5.10) and $\delta R' = 0.4$ fm one arrives at $\delta \sigma_{coh} = 0.37$ b, which is considerably higher than $\delta \sigma_s = 0.03$ b and implies $\Delta \sigma_s \approx 0.37/2.06$ or 18%. Comparison with other results is given in Table 5.2

Table 5.2: $^{55}\text{Mn}(n,\text{el})$ thermal cross section and its uncertainty from various sources compared to uncertainty propagated from the scattering radius.

Source	$\sigma_n(E_{th})$	$\Delta \sigma_n(E_{th})$	Comment
Atlas	2.06 b	1.5%	Atlas: $\sigma_s = 2.06 \pm 0.03$ b ^{*)}
ENDF/B-VII.0	2.16 b		Covariances not provided
ENDF/A	2.12 b	2%	New evaluation by ORNL in 2008
Low-fidelity		2.5%	Based on Atlas, adjusted to VII.0
From R'		18%	Based on $R' = 4.5 \pm 0.4$ fm (Atlas)

^{*)} Atlas uses notation σ_s for the free thermal scattering cross section.

Chapter 6

Correlation coefficients

In Chapters 2-5 we derived the formalism for obtaining uncertainties of cross sections averaged over suitable energy bins. This formalism uses available resonance parameter uncertainties, but it can not be fully applied unless correlations between resonance parameters in the energy bins were established. Once this is done and the cross section uncertainties are computed, they constitute diagonal terms of the covariance matrix. Then, one must establish correlation coefficients between the energy bins to get off-diagonal terms of the full covariance matrix.

Before explaining how we arrived at default values of correlation coefficients we make some more general observations.

6.1 Notation

Consider a set of parameters p_j with the absolute uncertainties (or variances) δp_j and relative uncertainties Δp_j . Then, correlation coefficient between parameters p_j and p_k is the normalized value of the off-diagonal term of the parameter covariance matrix,

$$\langle \Delta p_j \Delta p_k \rangle = \frac{\langle \delta p_j \delta p_k \rangle}{\delta p_j \delta p_k}. \quad (6.1)$$

Consequently, correlation coefficients have values between -1.0 and +1.0.

Throughout this paper we use two different notations for correlation coefficients. In the formalism developed in previous Chapters we resorted to notation

that stressed the link between correlation coefficients and relative uncertainties. Therefore, correlation coefficients were denoted as

$$\langle \Delta p_j \Delta p_k \rangle.$$

To make correlation coefficients intuitively more understandable we will use also equivalent notation

$$\text{corr}(p_1, p_2) = \langle \Delta p_1 \Delta p_2 \rangle.$$

6.2 Transmission and capture measurements

In general, correlations are determined by experimental conditions and data reduction procedures. Thus, if one wants to assess correlations one should start with analysis of experiments that supplied the data used by evaluators. Two different measurements, transmission and capture, are needed for determining resonance parameters.

In transmission measurement one measures attenuation of neutron flux caused by elastic scattering and capture (fission). A characteristic feature of measured transmission data are dips which refer to individual resonances. One measures with sample-out and sample-in using samples with different thickness to determine flux attenuation for thin samples. The baseline shift in attenuated neutron flux is due to potential scattering. For thin samples transmission dip areas are proportional to

$$A \propto g\Gamma_n. \quad (6.2)$$

Radiative capture measurements supply the remaining information. Measured data display peaks, with capture peak areas proportional to

$$A_\gamma \propto g\Gamma_n \frac{\Gamma_\gamma}{\Gamma}. \quad (6.3)$$

As usual, there are two types of uncertainties in these measurements, statistical and systematic. This latter uncertainty is critical for long-range correlations. Systematic uncertainty is caused by a number of effects, such as weighting function, normalization to standards, neutron flux determination, sample condition, detector efficiency, dead-time corrections, *etc.* Systematic uncertainties lead to positive correlation between resonances.

Data reduction procedures include number of steps, such as background subtraction, calibration, correction for attenuation in the sample, correction for multiple neutron scattering and others. All these effects lead to positive correlation between resonances.

Assume, for example, that the data reduction involved subtraction of a common background $b \pm \delta b$ and multiplication by a calibration factor $c \pm \delta c$. This means that the data reduction recipe to get count α_j from the raw count a_j with the statistical uncertainty $\pm \delta a_j$ was

$$\alpha_j = (a_j - b)c. \quad (6.4)$$

Then, the covariance matrix elements can be obtained as

$$\langle \delta \alpha_j \delta \alpha_k \rangle = \left\langle \left(\frac{\partial \alpha_j}{\partial a_j} \delta a_j + \frac{\partial \alpha_j}{\partial b} \delta b + \frac{\partial \alpha_j}{\partial c} \delta c \right) \left(\frac{\partial \alpha_k}{\partial a_k} \delta a_k + \frac{\partial \alpha_k}{\partial b} \delta b + \frac{\partial \alpha_k}{\partial c} \delta c \right) \right\rangle, \quad (6.5)$$

where sensitivities are

$$\frac{\partial \alpha_j}{\partial a_j} = c, \quad \frac{\partial \alpha_j}{\partial b} = -c \quad \text{and} \quad \frac{\partial \alpha_j}{\partial c} = a_j - b. \quad (6.6)$$

Individual components of Eq. (6.4) are uncorrelated, therefore, all cross terms on the right-hand side of Eq. (6.5) can be neglected giving

$$\langle \delta \alpha_j \delta \alpha_k \rangle \approx c^2 \delta_{jk} (\delta a_j)^2 + c^2 (\delta b)^2 + (a_j - b)(a_k - b) (\delta c)^2, \quad (6.7)$$

where δ_{jk} is the Kronecker delta. This expression makes it clear that the off-diagonal terms of the covariance matrix and hence also correlation coefficients due to data reduction are indeed positive. It also shows how difficult is to determine actual values of correlation coefficients without detailed information about systematic uncertainties and data reduction procedure.

6.3 Default values of correlation coefficients

Difficult part of establishing correlation coefficients in our procedure consists in the fact that they are not available in Atlas. Making their plausible estimate is therefore one of the most important issues that an evaluator must resolve. This holds for both MF33 and MF32 approach and the issue cannot be avoided.

According to our formalism one has to specify the values of several distinctive types of correlations:

- Correlations within a single resonance,
- Correlations between resonances in the energy bin,
- Correlation between potential scattering and resonance scattering,
- Correlations between energy bins,
- Correlation between thermal region and resonance region.

A summary of the default values of the correlation coefficients adopted in the present work is given in Table 8.6. A justification for these values is discussed in the following subsections.

Table 6.1: Default values of correlation coefficients (range -1.0 to +1.0) used in the present work.

No.	Type	Quantity	Default
1	Single resonance	$\text{corr}(\Gamma_n, \Gamma_\gamma)$	0.0
2	Resonance-resonance	$\text{corr}(\Gamma_{\gamma 1}, \Gamma_{\gamma 2})$	0.5
3		$\text{corr}(\Gamma_{n1}, \Gamma_{n2})$	0.5
4		$\text{corr}(\Gamma_{n1}, \Gamma_{\gamma 2})$	0.0
5	Pot. scattering-resonance	$\text{corr}(R', \Gamma_n)$	-0.5
6	Bin-bin	$\text{corr}(\bar{\sigma}_{\gamma 1}, \bar{\sigma}_{\gamma 2})$	0.5
7		$\text{corr}(\bar{\sigma}_{n1}, \bar{\sigma}_{n2})$	0.5
8	Thermal-resonance	$\text{corr}(\sigma_\gamma^{th}, \bar{\sigma}_\gamma)$	0.0
9		$\text{corr}(\sigma_n^{th}, \bar{\sigma}_n)$	0.0
10	Cross-correlation	$\text{corr}(\sigma_n^{th}, \sigma_\gamma^{th})$	0.0
11		$\text{corr}(\sigma_n^{res}, \sigma_\gamma^{res})$	-0.5

6.3.1 Single resonance

There is only one correlation of interest in this category, $\text{corr}(\Gamma_n, \Gamma_\gamma)$. It is difficult to assign this correlation properly unless one has sufficient knowledge about the evaluation procedure used to obtain individual resonance parameters that constitute the basis for data in the Atlas. If the kernel approach was used, then this correlation should be negative. It may, however, be also positive due to experimental

procedure whereby neutron sensitivity corrections is not properly accounted for.

In view of these ambiguities our default value for this correlation was set to 0.

6.3.2 Resonance - resonance

Under this category three correlations should be considered:

- $\text{corr}(\Gamma_{\gamma 1}, \Gamma_{\gamma 2})$. Due to systematic uncertainties and data reduction discussed above this correlations should be positive with values possibly close to 1. This is in line with the need to prevent decline of uncertainties in multigroup representation, which is deemed to be unphysical.

Default value for this correlation was set to 0.5.

- $\text{corr}(\Gamma_{n1}, \Gamma_{n2})$. The same arguments apply as for $\text{corr}(\Gamma_{\gamma}, \Gamma_{\gamma})$ correlations.

Default value for this correlation was set to 0.5.

- $\text{corr}(\Gamma_{n1}, \Gamma_{\gamma 2})$. In accordance with the argument applied for a single resonance we assume that this correlation can be neglected.

Default value for this correlation was set to 0.

6.3.3 Potential scattering - resonance scattering

Potential scattering is determined by the scattering radius R' , while resonance scattering is driven by Γ_n . Therefore, the correlation coefficient under discussion is $\text{corr}(R', \Gamma_n)$. We note that R' remains fairly constant as a function of energy and therefore potential scattering is bringing long-range correlation to elastic scattering.

Both R' and Γ_n can be derived from transmission measurements. One can argue that a negative correlation does exist between the potential scattering radius and neutron widths of resonances. The point is that increasing R' implies decrease in $g\Gamma_n$ and *vice versa*, while still preserving the same transmission. Similar argument can be made on the basis of Eq. (2.23) which shows that the average scattering cross section is sum of potential and resonance scattering, implying

negative correlation between the two terms and hence between R' and Γ_n . The magnitude of the correlation coefficient can vary from -1 to 0, depending on the quality of the data.

In the thermal energy region, the relation of the coherent scattering amplitude in terms of the potential scattering radius and the resonance parameters shows that there can be positive or negative correlation between R' and Γ_n . This depends on whether the resonance term in Eq. (5.7) is positive or negative, *i.e.*, whether the effect of the combined resonance terms from the positive energy resonances dominate over those of the bound levels or not.

In 2010, CSEWG extended ENDF-6 format by inclusion $\Delta R'$ under assumption that there is no correlation between R' and any of the resonance parameters. Provision was made to allow for such correlations in the future.

Default value for this correlation was set to -0.5.

6.3.4 Energy bin - energy bin

According to our procedure, the evaluator should first establish suitable energy bins (typically 10-15) over the whole resonance region. Resonance-resonance correlations within each bin were discussed above. What remains to be determined are correlations between these energy bins. These are correlations of the type $\text{corr}(\bar{\sigma}_{\gamma 1}, \bar{\sigma}_{\gamma 2})$ and $\text{corr}(\bar{\sigma}_{n1}, \bar{\sigma}_{n2})$.

Default value for each of these two correlations was set to 0.5.

6.3.5 Thermal region - resonance region

We treat thermal region and resonance region separately. This is justified by the fact that in most cases thermal values are measured independently from resonance quantities. This is true for both capture and elastic scattering, implying that in our approximation there is no correlation between these two regions. We note that in the evaluation of resonance parameters used in Atlas in many cases there is anti-correlation.

Default value for each of these two correlations was set to 0.

6.3.6 Cross-correlations

In principle there are correlations between different reaction channels, in our case between capture and elastic scattering. These cross-correlations can be different for thermal and resonance region.

Thermal region

In the thermal region elastic scattering cross sections are mostly determined by coherent scattering length measurements [1]. These are entirely independent from capture cross section measurements. Hence, related cross-correlation coefficient should be zero.

Default value for cross-correlation in the thermal region was set to 0.0.

Resonance region

In the resonance region elastic scattering cross sections are determined as difference between transmission and capture measurements. Hence, related cross-correlation coefficient should be negative. Since we are unable to establish its value precisely, our estimate is -0.5. In practice, in many cases elastic scattering cross sections are much larger than capture cross sections and impact of the correlation is small.

Default value for cross-correlation in the resonance region was set to -0.5.

Chapter 7

Resonance covariance module in EMPIRE

The formalism developed in this report should be incorporated into the resonance covariance module of the evaluation code EMPIRE [18] as an option for MF33 covariances rather than MF32. The MF33 option would offer several distinct advantages:

- More transparent results in terms of uncertainty step function, implying simple adjustment of uncertainties in the thermal region and incorporation of $\Delta R'$.
- No need to harmonize data in MF2 file with MF32 file and bypassing dependence on the processing codes with continuing issues in processing MF32 data.
- Better control over resonance-resonance correlations and prevention of uncertainty decline at higher resonance energies due to collapsing of many resonances into broad energy groups.

7.1 Functionalities

The resonance covariance module should offer the following functionalities:

1. Analysis of input. Easy inspection of input from Atlas that would allow basic analysis of these data, identification of missing data and determination

of the resonance energy range to be included into further evaluation by the module.

2. Computing kernels and group cross sections. Module should compute capture kernel and elastic scattering kernel along with related average cross sections for single resonances. Furthermore, it should compute capture and elastic cross sections in broader energy groups and compare them with multigroup cross sections produced by NJOY in order to judge whether kernels represent suitable approximation of group cross sections. We assume that there should be no problem with capture and fission (though interference effects in fission may appear to be challenging), while elastic scattering may cause certain difficulties which should be identified.
3. Computing cross section uncertainties. These should be computed from resonance parameter uncertainties for single resonances, followed by uncertainties of group cross sections composed of contributions from many resonances.
4. Analysis of integral quantities. The module should compute integral quantities (thermal, resonance integrals, Maxwellian average cross sections) including their uncertainties. It should allow comparison of data produced by EMPIRE with other sources of information, followed by improved evaluation.
5. Documentation. Module should keep reasonable track about the evaluation process and produce meaningful report in the form of MT451. This process should be automatized, similar to what has already been implemented as a part of evaluation of MF3 data in the fast neutron region.

7.2 Evaluation procedure

Basic steps of implementation the proposed kernel procedure can be formulated as follows:

1. Examine thermal cross sections and their uncertainties in Atlas, including dispersion with ENDF/B-VII.0 and other libraries. The goal is to determine thermal capture and elastic cross section uncertainties to be adopted in the present work.

2. Examine availability of resonance parameter uncertainties in Atlas and determine the range of applicability of kernel formalism. In doing so attention should be paid to the following quantities:
 - ΔE_0 : these uncertainties are usually small and well known;
 - ΔJ : spins are sometimes not determined for s-wave resonances, quite often for much weaker p-wave resonances and likely not at all for d-wave resonances \Rightarrow provision should be made to take related uncertainties into consideration, one possibility being estimate uncertainty by Monte Carlo simulation of spin assignment;
 - $\Delta \Gamma_n$: these uncertainties are important, it is difficult to estimate unknown values \Rightarrow energy range of availability should be carefully determined;
 - $\Delta \Gamma_\gamma$: these uncertainties are important, often one can estimate missing values by using average values \Rightarrow energy range should be carefully determined;
 - ΔA_γ : often capture kernels are available and provide an alternative way of producing covariances \Rightarrow energy range should be carefully determined.
 - $\Delta R'$: this uncertainty is important for elastic scattering and it might represent dominant contribution to elastic scattering cross section uncertainty at high energies \Rightarrow values in Atlas should be carefully examined.

3. Determine energy bins independently for capture and elastic scattering. These bins would define grouping of resonances. The number of energy bins is guided by user needs. Thus for example, nuclear critical safety users work with 44-energy groups in 10^{-5} eV - 20 MeV range. Fast reactor users prefer 33-energy group structure, with 14 energy groups in about 100 eV - 100 keV range.
 - Compute average cross sections in these energy bins within the kernel approximation and compare them with the values obtained by processing ENDF-6 formatted file.
 - If agreement is not satisfactory modify the energy bins to reach better accord with the values computed from kernels. This would enhance confidence in adopted binning.

4. Compute capture and elastic cross section uncertainties for these energy bins. These uncertainties would constitute diagonal terms of the covariance matrix.
5. Estimate correlations to get off-diagonal terms of the correlation matrix.

Chapter 8

Application to ^{55}Mn

It remains to be shown how the proposed formalism can be actually implemented. As an example we have chosen ^{55}Mn . The reason for this selection is that covariances for $^{55}\text{Mn}(n,\gamma)$ and $^{55}\text{Mn}(n,e1)$ cross sections in the resonance region were studied to some length using an alternative MF32 approach [19]. This allows us to compare the present formalism with MF32 results.

Shown in Fig. 8.1 are ^{55}Mn capture and elastic cross sections in the thermal and resonance region using evaluated data from ENDF/B-VII.0 which were Doppler-broadened to 300 K. The figure illustrates basic features of these cross sections. Among them is clear $1/v$ dependence for capture in the thermal region and fairly constant elastic cross sections in the range of about 10^{-2} eV to 10 eV. One can also see considerable differences in the shape of these cross sections at higher energies, while capture falls rapidly, scattering in the resonance region initially goes down with the energy and then remains approximately constant. These cross sections have different pattern, suggesting that binning should be done independently for capture and elastic.

Fig. 8.2 shows more details in the resonance region which in ENDF/B-VII.0 extends up to 100 keV. Average cross sections obtained by processing with the processing code NJOY can be seen in Fig. 8.3. This figure makes it clear that capture cross sections are 2-3 orders of magnitude smaller than elastic scattering.

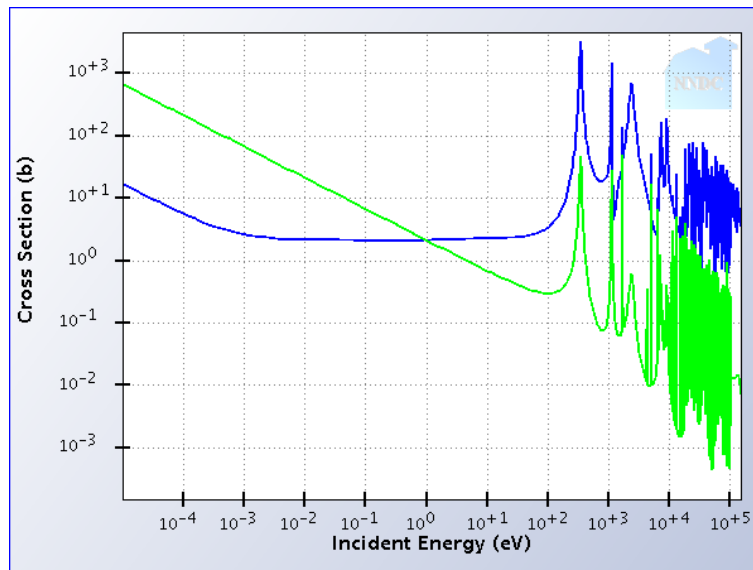


Figure 8.1: ^{55}Mn capture (green) and elastic (blue) cross sections in the thermal and resonance region. Data taken from ENDF/B-VII.0, produced by the NNDC retrieval and plotting system Sigma. Doppler-broadening to 300K leads to characteristic increase of elastic scattering at the lowest energies.

8.1 ^{55}Mn uncertainty data in Atlas

8.1.1 Thermal values

^{55}Mn thermal cross section uncertainties are given in Table 8.1. We note that the capture uncertainty, 0.37%, is considered to be too optimistic. Thus, 0.8% was recommended by reviewers of IRDF-2002 dosimetry file, and Derrien *et al.* [20] in 2008 reported 0.9%, we adopted 0.8%.

Dispersion in thermal elastic cross sections considerably exceeds the Atlas value of 1.5% and we adopted 3% in order to better comply with ENDF/B-VII.0 as well as Derrien'2008 which will likely be adopted by ENDF/B-VII.1.

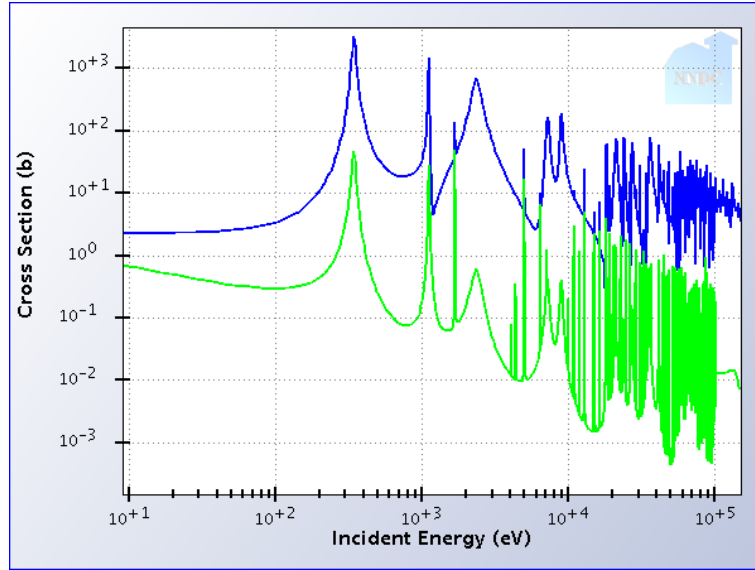


Figure 8.2: ^{55}Mn capture (green) and elastic (blue) cross sections in the resonance region. Data taken from ENDF/B-VII.0, produced by the NNDC retrieval and plotting system Sigma.

Table 8.1: ^{55}Mn thermal capture and elastic cross sections and uncertainties in barns. Shown are values given in ENDF/B-VII.0 (2006), Atlas (2006), and Derrien (2008) [20].

	VII.0	Atlas	Δ	Δ	Derrien	Δ	Δ	Adopted
	b	b	b	%	b	b	%	%
$\sigma_{\gamma}(E_{th})$	13.4	13.36	0.05	0.37%	13.27	0.12	0.9%	0.8%
$\sigma_n(E_{th})$	2.17	2.06	0.03	1.50%	2.12	-	-	3%

8.1.2 Resonance values

Resonance parameter uncertainties for ^{55}Mn available in Atlas [1] are summarized in Table 8.2. The resolved resonance region extends up to $E_0^{\max} = 208$ keV. The uncertainties of the resonance energies, ΔE_0 , are small, they increase with the energy, starting from about 0.1% and rising to about 0.3%. Spins of s-waves are known in the entire energy range, meaning that $\Delta J_{l=0} = 0$. However, this is not the case for p-waves, these spins are known in just a few instances. The uncertainties

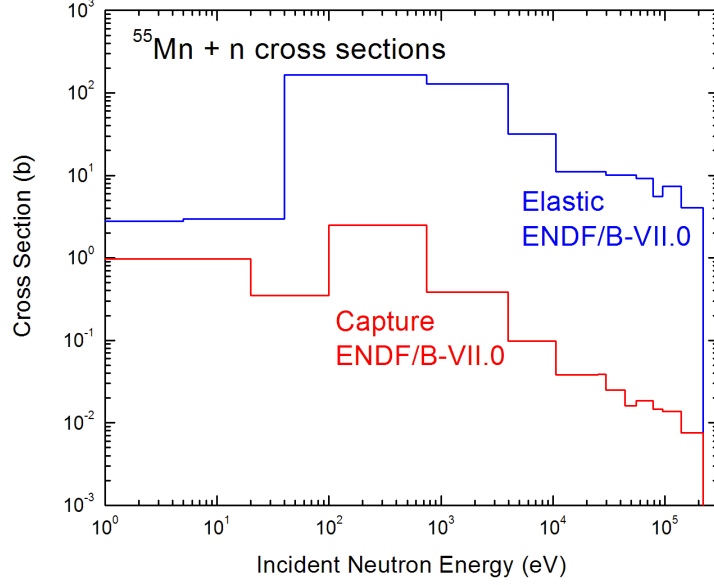


Figure 8.3: ^{55}Mn capture (red) and elastic (blue) from ENDF/B-VII.0. Group structure for NJOY processing is chosen to match energy binning adopted in the present work and discussed later in the text.

Table 8.2: Availability of ^{55}Mn resonance parameter uncertainties in Atlas. Shown are upper E_0 values for which $\Delta\Gamma_n$, $\Delta\Gamma_\gamma$ etc are known. Also given are % uncertainties for average s- and p-wave radiative widths, $\langle\Delta\Gamma_{\gamma 0}\rangle$ and $\langle\Delta\Gamma_{\gamma 1}\rangle$.

Nucleus	E_0^{\max}	ΔE_0	$\Delta J_{l=0}$	$\Delta J_{l=1}$	$\Delta\Gamma_n$	$\Delta\Gamma_\gamma$	ΔA_γ	$\langle\Delta\Gamma_{\gamma 0}\rangle$	$\langle\Delta\Gamma_{\gamma 1}\rangle$
	keV	E_0^{\max}	E_0^{\max}	E_0^{\max}	E_0^{\max}	E_0^{\max}	E_0^{\max}	%	%
^{55}Mn	208	208	208	0 ¹⁾	208	112 ²⁾	-	20	25

¹⁾ Spins of p-waves are virtually undetermined.

²⁾ There are gaps in $\Delta\Gamma_\gamma$, to be filled-in by average uncertainty values.

of neutron widths, $\Delta\Gamma_n$, are known in the entire resolved resonance region up to 208 keV. Uncertainties of radiative widths are known up to 112 keV only, implying that one must fully resort to average uncertainty values, $\langle\Delta\Gamma_{\gamma 0}\rangle$ and $\langle\Delta\Gamma_{\gamma 1}\rangle$, at

higher energies. As there are quite a few gaps in $\Delta\Gamma_\gamma$ below 112 keV, these gaps should be filled-in by the average values as well. We note that capture kernels are not given in Atlas for ^{55}Mn .

In order to get better feeling about the number of resonances we are dealing with, summary of ^{55}Mn resonances (g.s. spin $I = 5/2$) is given in Table 8.3. Atlas lists 170 resonances up to 207.7 keV, with $\Delta\Gamma_n$ and $\Delta\Gamma_\gamma$ provided up to $E_0 = 111.76$ keV. There are 148 resonances in this energy range, with $\Delta\Gamma_n$ and $\Delta\Gamma_\gamma$ known simultaneously for 71 resonances of which 50 are s-waves and 21 p-waves. These are strong or fairly strong resonances that should be included into our consideration, the remaining resonances being mostly weak. For the first 30 resonances the uncertainties are known for 12 resonances, of which 9 are s-waves and 3 are p-waves.

Table 8.3: Summary of ^{55}Mn resonances.

Energy range	Number of resonances	Known $\Delta\Gamma_n$	Known both $\Delta\Gamma_n, \Delta\Gamma_\gamma$	s-wave	p-wave
0 - 207.7 keV	170	168	71	50	21
0 - 111.7 keV	148	146	71	50	21
0 - 23.6 keV	30	29	12	9	3

Scattering radius

Uncertainty of scattering radius, $\Delta R'$, is of considerable importance particularly at higher energies where potential scattering likely represents dominant contribution to elastic scattering. It is important to realize the values of R' and $\Delta R'$ provided in Atlas are in general derived from the data in the thermal region. In the case of ^{55}Mn this gives $R' = 4.5 \pm 0.4$ fm or 8.9%.

What we need, however, is not the scattering radius uncertainty at the thermal energy, but $\Delta R'$ in the resonance region. In general, R' is energy-dependent quantity. Therefore, one should be cautious extrapolating the thermal value to resonance energies that extend to about 200 keV. To account for the lack of actual knowledge of $\Delta R'$ in the resonance region we decided to adopt twice the value

determined at the thermal energy, *i.e.*, 17.8%. As shown in Table 8.4 this uncertainty complies with fairly large discrepancy between absolute values of R' in the ENDF/B-VII.0 library and Atlas of Neutron Resonances.

Table 8.4: Scattering radius and its uncertainty for ^{55}Mn .

ENDF/B-VII.0	A t l a s			Adopted
R'	R'	$\Delta R'$	$\Delta R'$	$\Delta R'$
fm	fm	fm	%	%
5.15	4.5	0.4	8.9	17.8

8.2 $^{55}\text{Mn}(n,\gamma)$ covariances

We proceed in three steps. First, we establish energy bins by suitably subdividing the entire resonance region, then determine correlations within these bins and compute uncertainties of average cross sections, and finally determine bin-bin correlations and construct a complete covariance matrix.

8.2.1 Energy binning

When doing energy binning an evaluator determines which resonances are put together and subsequently handled as a single entity. One proceeds iteratively, starts with estimates, computes average cross sections from kernels and compares these approximate values with correct values obtained by processing MF2 in MLBW representation with NJOY. Once good agreement is reached the binning is considered to be completed.

The outcome of our procedure is shown in Fig. 8.4. The results in the resonance region are complemented with thermal values obtained directly from the thermal cross section and $1/v$ law. One can see that pretty good agreement was achieved in the whole energy range, giving confidence that our approximation is sound.

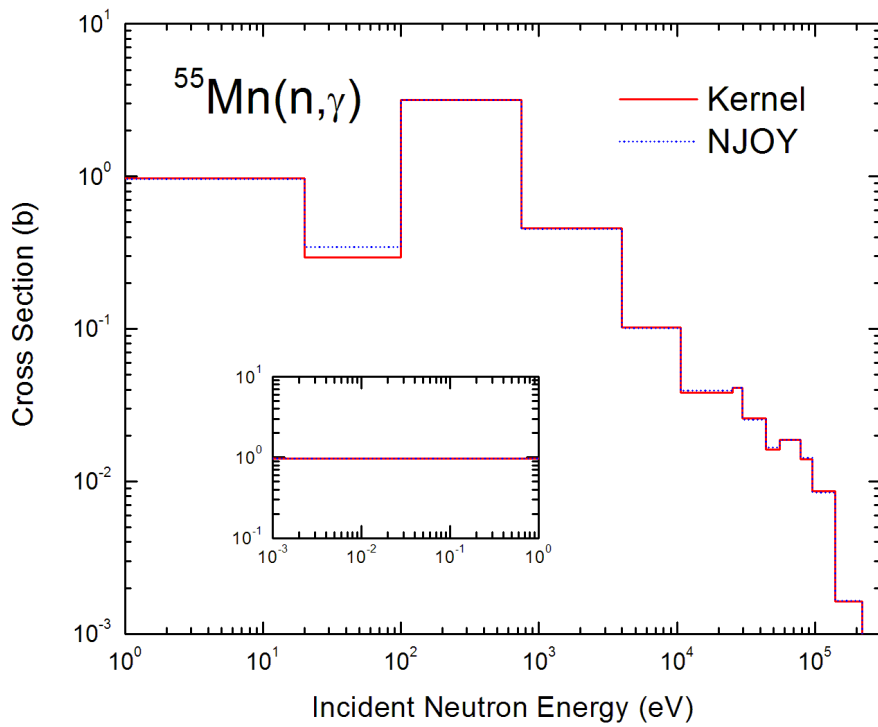


Figure 8.4: Comparison of average cross sections for ^{55}Mn capture obtained from kernels (above 100 eV) and from NJOY in the whole energy range. Below 100 eV the kernel values are obtained from $1/v$ dependence normalized to thermal cross section. Shown in the insert is the energy region from 10^{-3} eV to 1 eV.

8.2.2 Uncertainties for capture

Relative uncertainties of average capture cross sections can be seen in Fig. 8.5. As already discussed the uncertainties depend on values of resonance-resonance correlations. We assumed that the correlations can be adopted uniformly for each energy bin and considered extreme values, fully correlated, $\text{corr}(\Gamma_\gamma, \Gamma_\gamma) = 1.0$ and $\text{corr}(\Gamma_n, \Gamma_n) = 1.0$, completely uncorrelated resonance parameters ($\text{corr} = 0$) and also intermediate correlation ($\text{corr} = 0.5$). One can see that at high energies the impact is strong and unless full correlation is considered, there is appreciable decline in relative uncertainties.

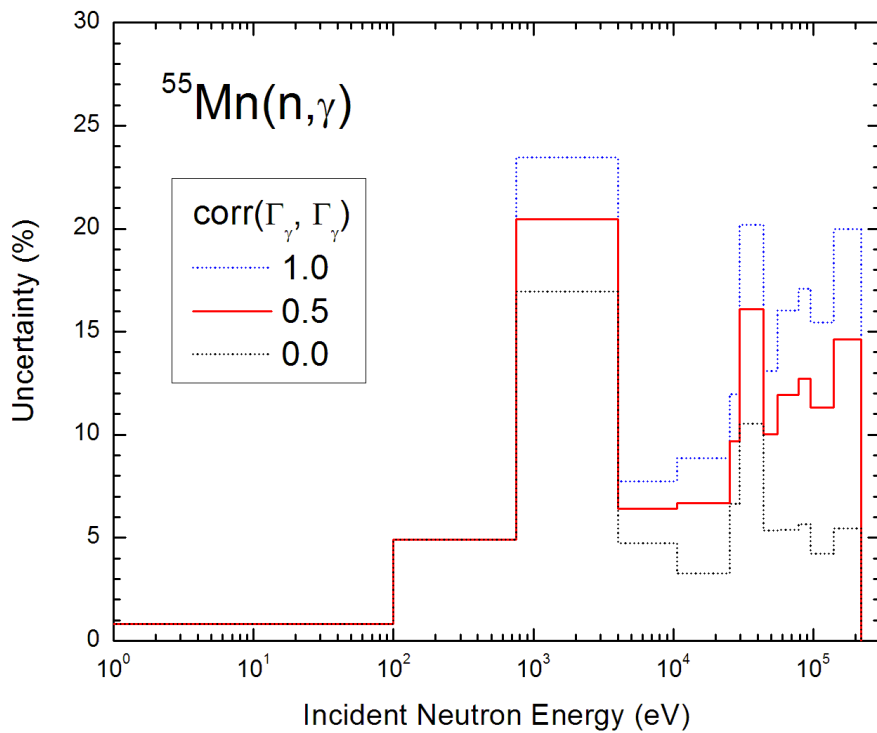


Figure 8.5: Relative uncertainties of average cross sections for ^{55}Mn capture. Shown are results for three different values of resonance-resonance correlation coefficients, $\text{corr}(\Gamma_\gamma, \Gamma_\gamma)$, applied uniformly within each energy bin. We note that impact of $\text{corr}(\Gamma_n, \Gamma_n)$ on capture is marginal.

8.2.3 Covariances for capture

Full covariance matrix was produced by using the above uncertainties, adding bin-bin correlation coefficients and converting this information into MF33 file. Then, NJOY was used to process the covariances into 33-group representation. This was done for three values of resonance-resonance and bin-bin correlation coefficients, namely 0.0, 0.5 and 1.0. All of these correlations were considered to be identical and they were thus applied uniformly across the whole resonance region. The results are shown in Fig. 8.6.

As expected the most conservative cross section uncertainties were obtained for fully correlated resonance parameters, while the other extreme of uncorrelated parameters leads to unrealistically low values. The intermediate approach seen at top right seems to be still reasonable and probably represents the preferable solution.

Formalism for Covariances in the Resonance Region

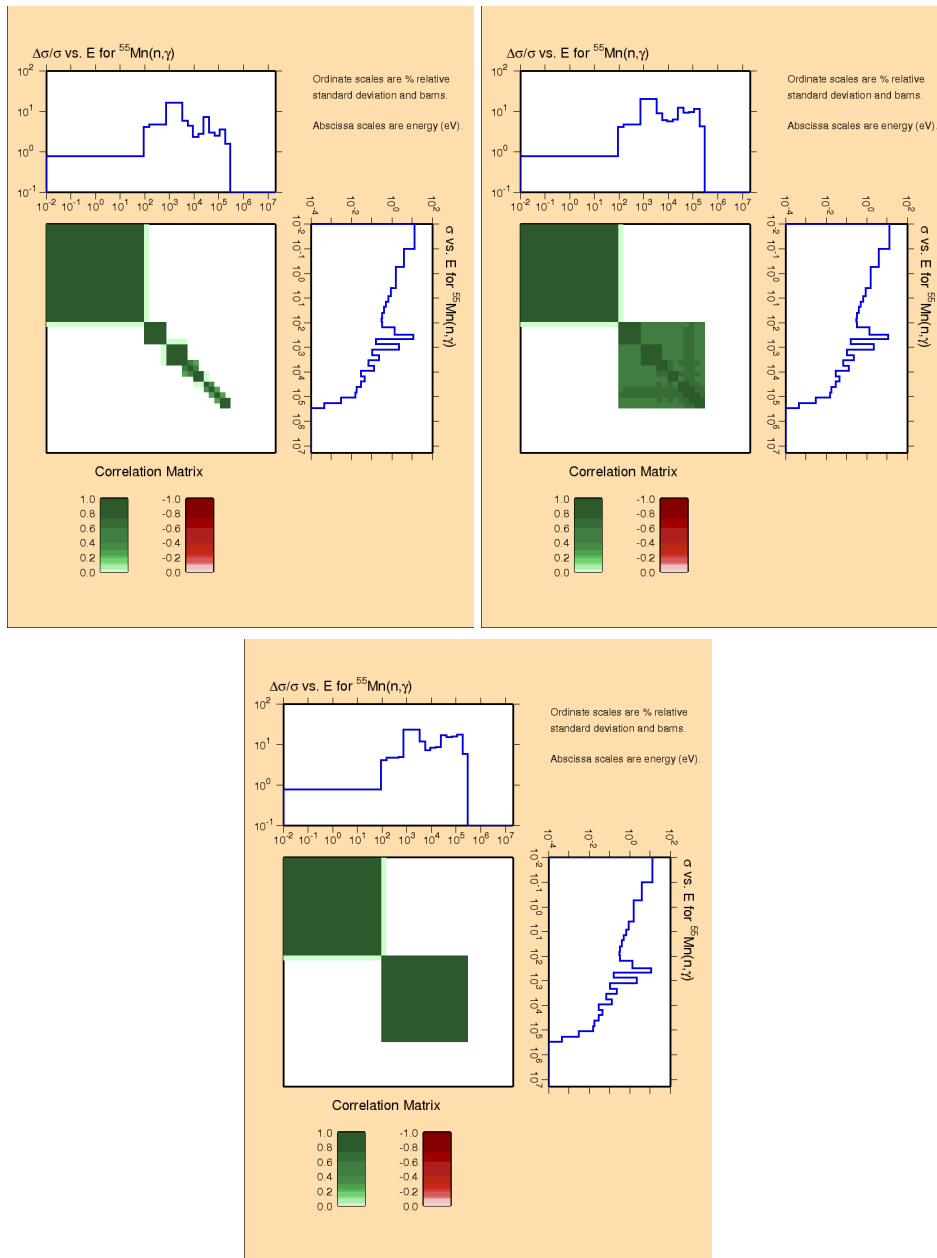


Figure 8.6: Covariances for ^{55}Mn capture in 33-energy groups for three values of resonance-resonance and bin-bin correlation coefficients: 0.0 (top left), 0.5 (top right) and 1.0 (bottom).

8.3 $^{55}\text{Mn}(n,\text{el})$ covariances

8.3.1 Energy binning

Similar to capture, as the first step one establishes suitable energy bins for resonances. We note that the shape of elastic cross section is more complicated due to presence of potential scattering, interference effects between potential and resonance scattering as well as resonance-resonance interference. Therefore, in general, one may end up with different binning than that established for capture. The results of our procedure can be seen in Fig. 8.7 which shows average elastic scattering cross sections. Approximate values obtained from kernels are compared with correct values produced by NJOY using MLBW representation. One can see that reasonable agreement was reached, suggesting that our approximation should be sound.

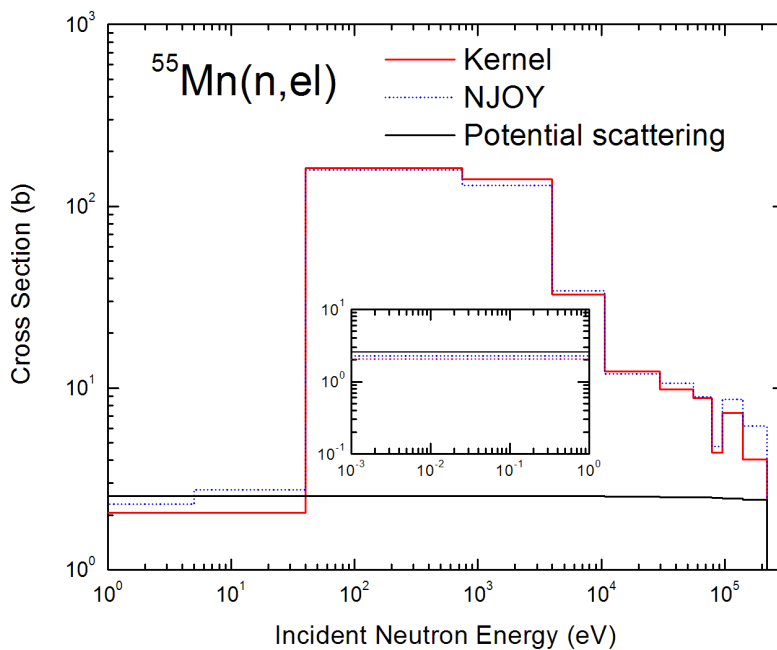


Figure 8.7: Comparison of average cross sections for ^{55}Mn elastic scattering obtained from kernels (above 40 eV) and from NJOY in the whole energy range. The kernel values in the thermal region (below 40 eV) were obtained directly from the thermal cross section. Shown in the insert is the energy region from 10^{-3} eV to 1 eV.

8.3.2 Uncertainties for elastic scattering

Relative uncertainties of average capture cross sections can be seen in Fig. 8.8. As already discussed these uncertainties depend on adopted values of resonance-resonance correlations, $\text{corr}(\Gamma_n, \Gamma_n)$ and $\text{corr}(\Gamma_\gamma, \Gamma_\gamma)$. Similar to capture we assumed that the correlations can be adopted uniformly for each energy bin. Considered were extreme values, fully correlated ($\text{corr} = 1$) and completely uncorrelated resonance parameters ($\text{corr} = 0$) and also intermediate correlation ($\text{corr} = 0.5$). One can see that at high energies the impact is strong and unless full correlation is considered, there is considerable decline in relative uncertainties.

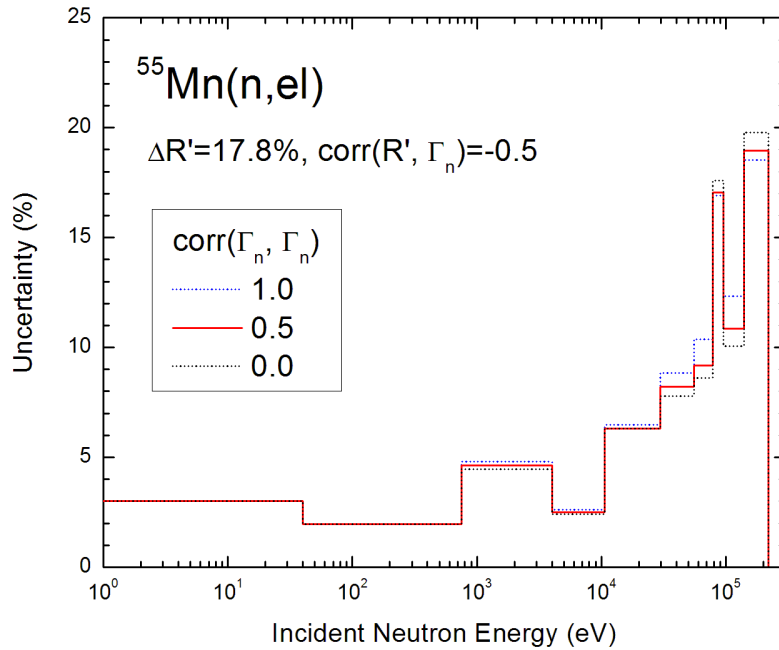


Figure 8.8: Uncertainties of average cross sections for ^{55}Mn elastic scattering. Shown are results for three different values of resonance-resonance correlation coefficients, $\text{corr}(\Gamma_n, \Gamma_n)$, adopted uniformly for each energy bin. We note that impact of $\text{corr}(\Gamma_\gamma, \Gamma_\gamma)$ on scattering is marginal.

It is instructive to illuminate contribution of scattering radius uncertainty, $\Delta R'$, to the uncertainty of the average elastic cross section. This is shown in Fig. 8.9, where we compare full elastic scattering uncertainties with those computed under

assumption that R' is known exactly. It is clear that within our formalism this has no impact on the thermal region. At low-energy resonances, where σ_n^{res} is much larger than $\sigma_n^{pot} = 2.54$ b, the impact of $\Delta R'$ is positive but small. At high energies, where σ_n^{res} becomes comparable to σ_n^{pot} , the scattering radius uncertainty increases the overall uncertainty quite considerably.

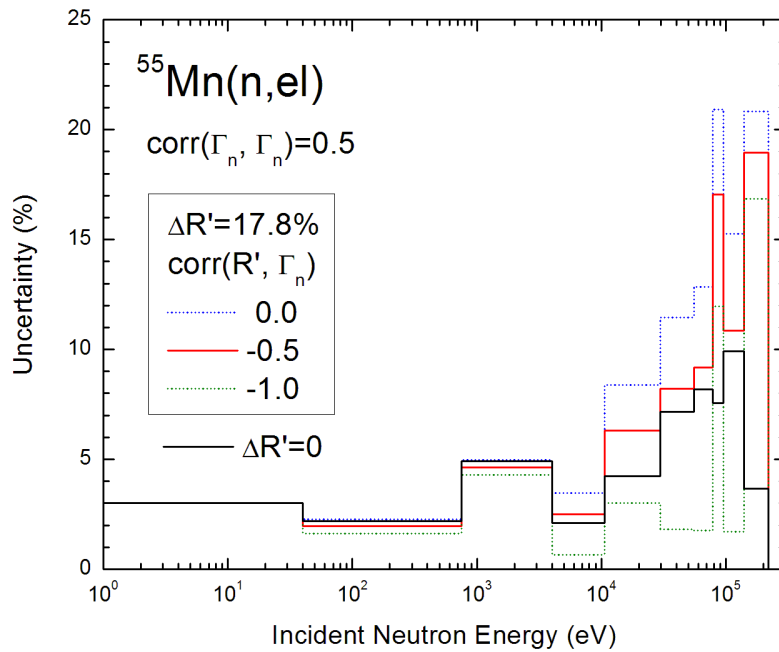


Figure 8.9: Uncertainties of average cross sections for ^{55}Mn elastic scattering for two scenarios of scattering radius uncertainty, $\Delta R'$. Used in both cases were default values of correlation coefficients, $\text{corr}(\Gamma_n, \Gamma_n) = 0.5$ and $\text{corr}(R', \Gamma_n) = -0.5$.

8.3.3 Covariances for elastic scattering

A full covariance matrix was produced by using the above uncertainties, adding bin-bin correlation coefficients and converting this information into MF33 file. Then, NJOY was used to process the covariances into 33-group representation. This was done for three values of resonance-resonance and bin-bin correlation coefficients, namely 0.0, 0.5 and 1.0. Each of these correlations was applied uniformly across the whole resonance region. The results are shown in Fig. 8.10.

As expected the most conservative cross section uncertainties were obtained for fully correlated resonance parameters, while the other extreme of uncorrelated parameters leads to unrealistically low values. The intermediate approach seen at top right seems to be still reasonable and is probably the preferable solution.

Formalism for Covariances in the Resonance Region

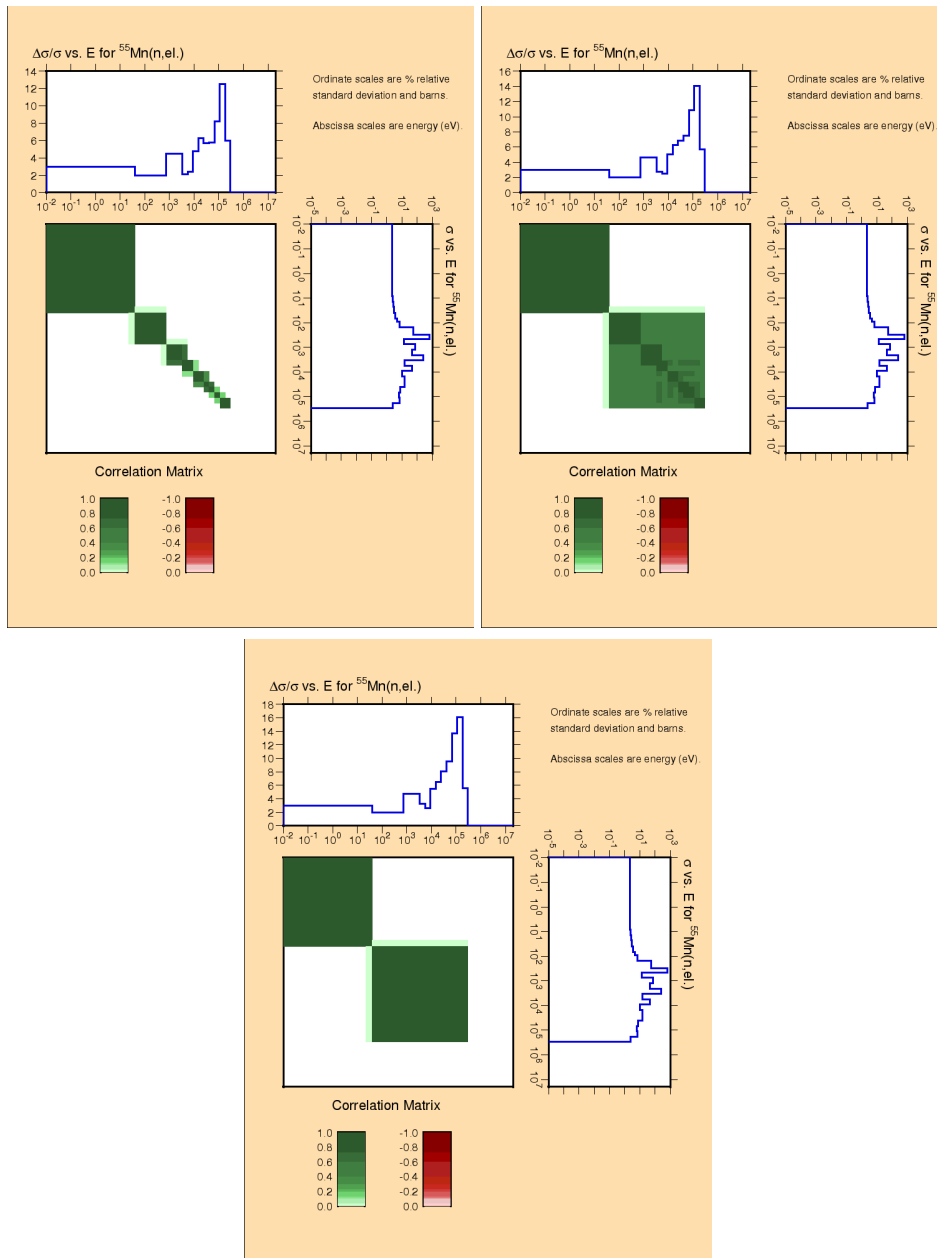


Figure 8.10: Covariances for ^{55}Mn elastic scattering in 33-energy groups for three values of resonance-resonance and bin-bin correlation coefficients: 0.0 (top left), 0.5 (top right) and 1.0 (bottom).

8.4 Comparison with MF32

Covariances for ^{55}Mn capture and elastic cross sections have also been estimated using the MF32 approach, which is an option in the covariance resonance module of the code EMPIRE [21]. MF32 approach uses resonance parameter information from the Atlas of Neutron Resonances to create the resonance parameter covariances. These are stored in file MF32 in accordance with the ENDF-6 formatting rules. The idea behind this approach is that the complex job of propagating MF32 covariances to cross section covariances is delegated to well established processing codes such as NJOY and PUFF.

8.4.1 Evaluation procedure

To create MF32, the resonance module reads information about all resonance parameters and uncertainties from the Atlas. Since the Atlas is based on experimental data, some data may be missing or incomplete. For example, spin assignments may be missing for some resonances, and uncertainties of the neutron scattering and radiative widths, $\Delta\Gamma_n$ and $\Delta\Gamma_\gamma$, may be missing especially for higher incident neutron energies and for weak resonances. The module therefore contains subroutines for assigning unknown spins as well as for estimating unknown resonance parameters and uncertainties. This is done as follows:

- Unknown spins are assigned by the code PTANAL using approach often adopted by evaluators of MF2 data [22]. The assignments are made statistically in accordance with spin distribution prescribed by nuclear level densities.
- Unknown radiative widths and their uncertainties were assumed to be equal to average values given in the Atlas.
- No attempt was made to assign unknown neutron widths and their uncertainties. This was the case for two resonances only, which were considered to be weak and removed from the analysis.

The resonance parameter uncertainties constitute diagonal terms of the resonance parameter covariance matrix. As for the non-diagonal terms, there is no information available in Atlas and these terms must be estimated. In the preferred representation of separating covariance matrix into uncertainties and normalized correlation matrix, the normalized correlation coefficients are subject to estimation. This was done as follows:

- Correlations from adjustment of thermal uncertainties. One of the problem faced by the evaluator is caused by the fact that uncertainties in Atlas are not internally harmonized. Thus, the uncertainties of thermal values readily available in Atlas do not agree with the uncertainties obtained from propagating resonance parameter uncertainties which in general provide higher thermal uncertainties. The challenge is that one should preserve thermal and resonance parameter uncertainties and yet to reach mutual agreement for thermal point. This is taken care of by the dedicated adjustment procedure that uses the generalized least-squares approach of the code KALMAN and assigns suitable correlations between negative and few initial positive resonances. In many cases this procedure ends up with anticorrelations that reduce contributions from resonances and produce desired thermal uncertainty.
- Resonance-resonance correlations. These are $\text{corr}(\Gamma_n, \Gamma_n)$, $\text{corr}(\Gamma_n, \Gamma_\gamma)$ and $\text{corr}(\Gamma_\gamma, \Gamma_\gamma)$ correlation coefficients. If these correlations are set to zero, then it would lead to reduction of uncertainties in the collapsing of cross sections to multigroup representation. This effect can be fairly strong at higher neutron resonance energies where energy grouping usually involves many resonances (see next section). In order to prevent this effect we assumed that the resonance-resonance correlation between neutron widths is 100% and also between radiative widths is 100%.
- Potential scattering. Potential scattering uncertainty can be taken into account via scattering radius, $R' \pm \Delta R'$, making use of recent (late 2009) extension of processing capabilities by both NJOY and PUFF codes. However, this extension was relatively simple and assumes that R' is not correlated with the resonance parameters. Even though it is in accordance with the extension of ENDF-6 formats adopted by CSEWG in November 2009, one clearly needs more sophisticated implementation. In view of this for the purposes of present exercise we did not take into account $\Delta R'$.

8.4.2 Results and discussion

⁵⁵Mn capture cross section uncertainties produced by the resonance module are shown in Fig. 8.11. The histograms were obtained by processing MF32 file with NJOY. The blue curve shows the uncertainty in a very fine group structure, while the other curves refer to 33-energy group structure for different correlations. The

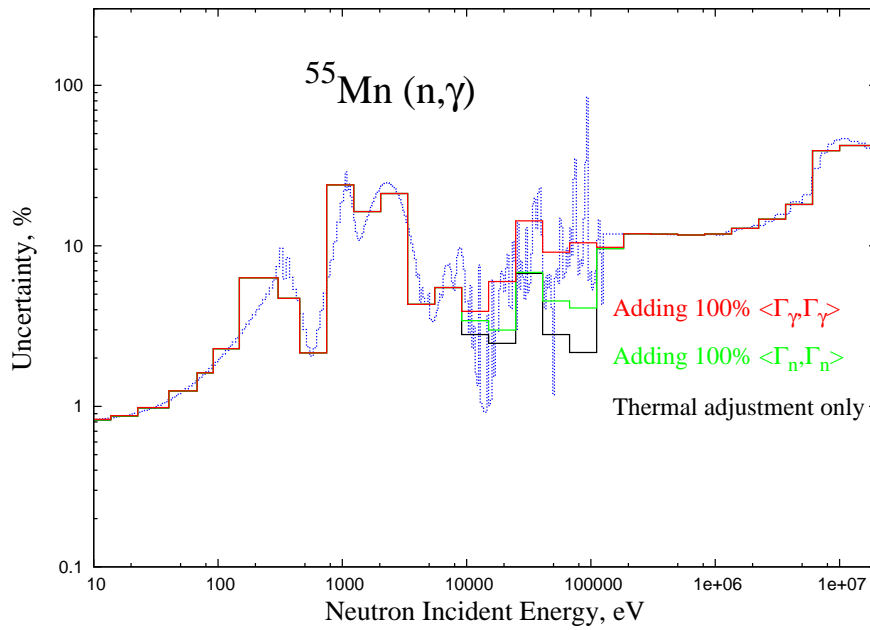


Figure 8.11: Cross section uncertainties for $^{55}\text{Mn}(n,\gamma)$ obtained from MF32 that extends up to 208 keV. Three different scenarios for resonance-resonance correlations were considered. Blue curve refers to fine group structure with just one or very few resonances per group which largely eliminates effect of correlations. Histograms refer to 33-energy group structure assuming full correlation between capture and neutron widths: black - no correlations, green - $\text{corr}(\Gamma_n, \Gamma_n) = 1.0$, red - $\text{corr}(\Gamma_\gamma, \Gamma_\gamma) = 1.0$. Fast neutron region is based on MF33 and it is shown for completeness.

black curve reflects no-correlation scenario and therefore uses only diagonal terms in the resonance parameter covariance matrix, the red curve assumes 100% correlations between Γ_γ for all resonances and similarly the green curve assumes 100% correlations between Γ_n .

As we can see, the 33-group uncertainties tend to decrease at higher incident neutron energies. This effect can be explained by rapidly increasing density of resonances: the grouped uncertainty of uncorrelated resonances is proportional to \sqrt{N} , with N being the number of strong resonances in the group. Preventing this decrease for capture cross sections was caused by assuming $\text{corr}(\Gamma_\gamma, \Gamma_\gamma) = 1.0$ between all resonances.

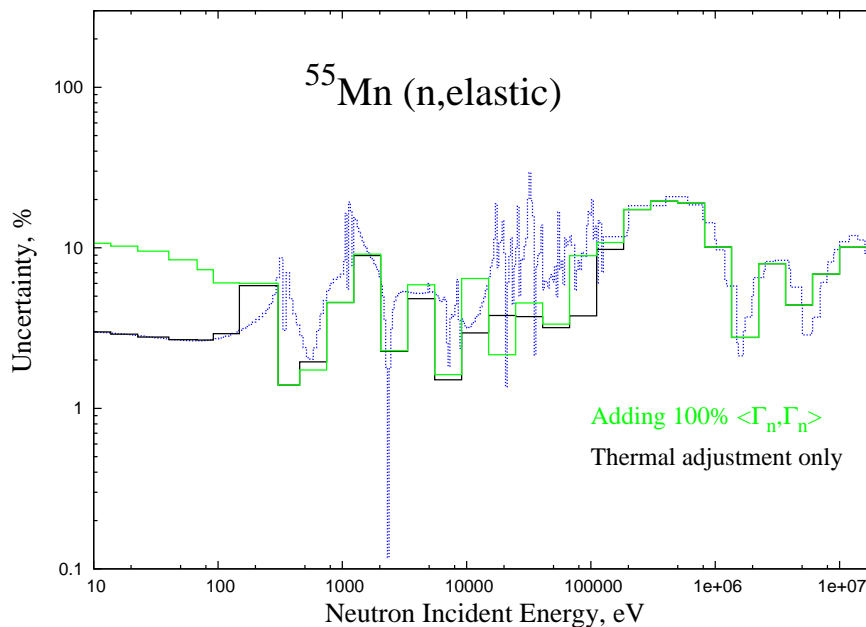


Figure 8.12: Cross section uncertainties for $^{55}\text{Mn}(n,\text{el})$ obtained from MF32 that extends up to 208 keV. Scattering radius uncertainty was not taken into account, *i.e.*, $\Delta R' = 0$. MF32 was processed by NJOY using fine group structure (blue curve) and 33-groups to illustrate collapsing effect ($\text{corr}(\Gamma_n, \Gamma_n) = 1.0$ - green, $\text{corr}(\Gamma_n, \Gamma_n) = 1.0$ - black). Fast neutron region is based on MF33 and it is shown for completeness.

Uncertainties for elastic scattering produced by MF32 can be found in Fig. 8.12, where $\Delta R'$ was assumed. Similar to capture, one would assume that $\text{corr}(\Gamma_n, \Gamma_n)$

= 1.0 would also exhibit strong impact. It appears, however, that this is not the case. Contribution from $\text{corr}(\Gamma_n, \Gamma_n) = 1.0$ ruined the thermal elastic scattering uncertainty by making it much higher than the value based on experimentally determined uncertainty. On the other hand, even though $\text{corr}(\Gamma_n, \Gamma_n) = 1.0$ resulted in some increase of uncertainties at higher energies, it was clearly insufficient to eliminate \sqrt{N} effect. We cannot provide plausible explanation for this behavior and cannot exclude bug in the processing codes.

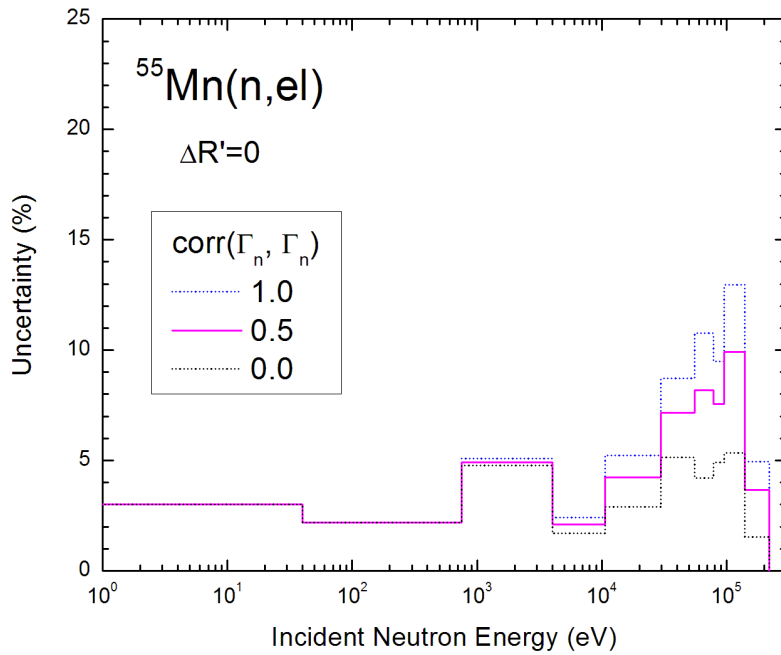


Figure 8.13: Relative uncertainties for $^{55}\text{Mn}(n,\text{el})$ based on the kernel approximation. Assumed was $\Delta R' = 0$ and three different values of $\text{corr}(\Gamma_n, \Gamma_n) = 1.0, 0.5$ and 0.0 .

$^{55}\text{Mn}(n,\text{el})$ uncertainties obtained from the kernel approach assuming $\Delta R' = 0$ are shown in Fig. 8.13 for comparison. We considered three scenarios for $\text{corr}(\Gamma_n, \Gamma_n)$, namely, 1.0, 0.5 and 0.0. One can see that impact of this correlation is within expectation. At the energy range of interest for comparing collapsing effect, about 20 keV - 100 keV, where kernel and MF32 regions overlap one can see that kernel with full correlation gives clearly higher uncertainties than MF32. Thus, kernel uncertainties are within 5-13%, while MF32 are within 2-9%. This again suggests that there might be possible issue in MF32 processing.

8.5 Comparison with ENDF/A

ENDF/A library contains candidate evaluations for inclusion into new release of ENDF/B library, in this case ENDF/B-VII.1. New ^{55}Mn evaluation was performed by Derrien *et al* [20, 23] who evaluated simultaneously MF2 and MF32 up to 122 keV by SAMMY. We retrieved the file from the NNDC GForge server on April 6, 2010, processed it using 33-group representation with the latest versions of NJOY and PUFF to check for possible processing issues.

Results are shown in Fig. 8.14. Capture uncertainties manifest notable differences at high energies. Thus, NJOY claims that they go up to 2.2%, while PUFF says that they go down to 0.6%. Elastic scattering uncertainties seem to agree fairly well except for notable difference in the 3rd group from the right.

8.5.1 $^{55}\text{Mn}(n,\gamma)$ uncertainties

Table 8.5: Comparison of uncertainties for $^{55}\text{Mn}(n,\gamma)$ and $^{55}\text{Mn}(n,\text{el})$. Given are values reported in PHYSOR'2008 [20], values obtained by processing ENDF/A file and present results.

Reaction	Energies keV	PHYSOR %	E N D F / A		Present %
			NJOY	PUFF	
(n,γ)	15 - 120	4.3 - 9.5	0.8 - 2.2	0.8 - 0.6	7 - 13
(n,el)	10 - 120	-	1 - 0.2	1 - 0.2	6 - 14

ENDF/A capture uncertainties can be seen in Fig. 8.14, top. We focus on uncertainties by PUFF since it is ORNL code and ENDF/A file was produced also by ORNL. Above about 10 keV uncertainties tend to decrease, from 0.8% to 0.6%. If correct, $^{55}\text{Mn}(n,\gamma)$ would be better determined than $\text{Au}(n,\gamma)$ standard known to about 1% at these energies [24]. Furthermore, uncertainties obtained by processing are in contradiction with results reported in PHYSOR'2008 [20] and also in MT451 description of ENDF/A file. These two sources make it clear that in the energy range of 15 keV - 120 keV capture uncertainty increases from about 4.3% to 9.5%. We believe that this issue points to lack of correlations in MF32.

Formalism for Covariances in the Resonance Region

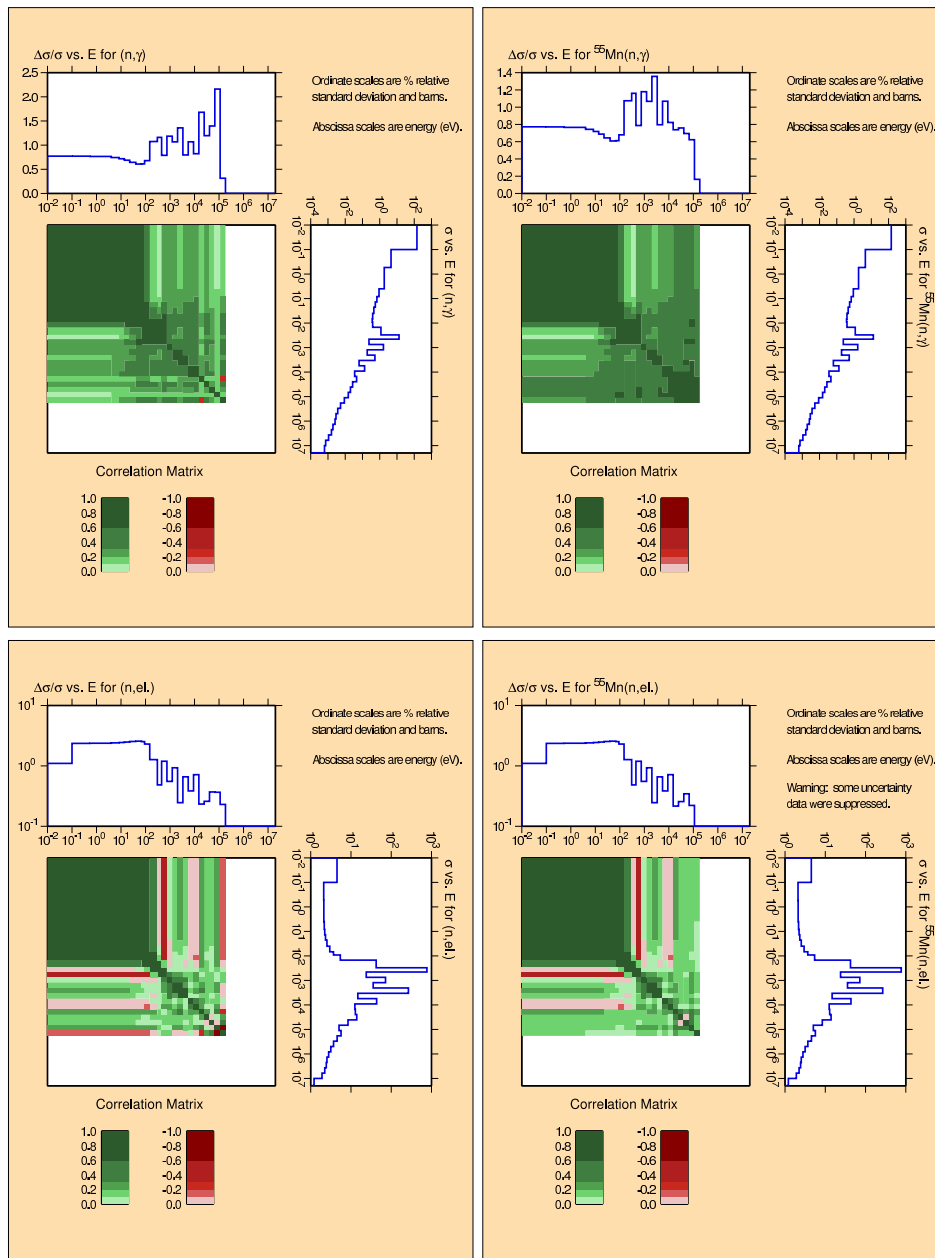


Figure 8.14: $^{55}\text{Mn}(n,\gamma)$ and (n,el) covariances in 33-groups obtained by processing ENDF/A file with the latest versions of NJOY (left) and PUFF (right). The difference in capture uncertainties at high energies is striking (top).

Our results for capture look more realistic, see Fig. 8.5. They comply with expected tendency of increasing uncertainties with the energy and are in better agreement with PHYSOR values, even though they are more conservative, see Table 8.5.

8.5.2 $^{55}\text{Mn}(n,\text{el})$ uncertainties

As shown in the bottom part of Fig. 8.14 ENDF/A elastic scattering uncertainties above about 1 keV tend to decrease, from 1% to as low as 0.2%. Again, if correct, $^{55}\text{Mn}(n,\text{el})$ would be better determined than C(n,el) standard which is known to about 0.5% in this energy range [24]. Thus, ENDF/A uncertainties for elastic scattering are unrealistically low. In addition, ENDF/A evaluation seems to suffer from two other issues. First, contribution from potential scattering has not been included at all. Second, there is again lack of resonance-resonance correlations.

Our results in the resonance region, see Fig. 8.8, look more realistic and comply with expected tendency of increasing uncertainties with energy. The difference with ENDF/A is quite dramatic, see Table 8.5 for quick comparison.

8.6 Final results

Recommended covariances for $^{55}\text{Mn}(n,\gamma)$ and $^{55}\text{Mn}(n,\text{el})$ are those shown in Figs. 8.6 and 8.10 top right.

8.6.1 Adopted correlation coefficients

The critical issue to be resolved in preparing covariances for ^{55}Mn is to answer a question about resonance-resonance correlations in any given energy bin (medium-range correlations) and, to less extend also about long-range bin-bin correlations. In the final analysis we adopted uniform value of 0.5 to all of them as shown in Table 8.6. The reasons for our selection are as follows:

- Capture uncertainties obtained in the latest analysis of Derrien *et al.* (Ref. [20], file included in ENDF/A) in the energy range of 15 keV - 120 keV increase gradually from 4.3% to 9.5%. These uncertainties exclude extreme values of the correlation coefficients, see Fig. 8.5, and are in line with our choice of 0.5.

- One should prevent decline of uncertainties in 33-group representation at the high end of the resonance region. Experimentalists would agree that such decline is not supported by experiments and our choice of 0.5 is preventing such decline.
- Our analysis suggests that the resonance-resonance correlations should be positive. This is due to systematic errors and data reduction. In the situation that we have no way to determine their actual values, to go mid-way to 0.5 seems to be a reasonable solution.
- For correlation between R' and Γ_n we adopted default value -0.5. This is in line with reasoning that σ_n^{pot} is anticorrelated with σ_n^{res} and having no detailed knowledge of the actual value of the correlation coefficient to go mid-way to -0.5 seems to be reasonable solution.
- For cross-correlation between elastic scattering and capture in the thermal region we adopted 0.0. This is in agreement with the fact that we use experimentally observed uncertainties determined independently.
- For cross-correlation between elastic scattering and capture in the resonance region we took into account the fact that $\sigma_n \gg \sigma_\gamma$. Therefore, practical impact of this correlation is negligible and for simplicity we adopted the value 0.0.

8.6.2 Quality assurance

The following tests of the final ^{55}Mn covariances were performed:

- Positive-definiteness of the covariance matrix. It was found that all eigenvalues are positive except of two tiny negative values for elastic and one zero for capture indicating that the matrix is suitable for practical applications.
- Relative uncertainties too low. Our covariances do not show unrealistically low uncertainties.
- Decline of relative uncertainties. Our covariances do not exhibit gradual decline of uncertainties with increasing resonance energy.

Table 8.6: Correlation coefficients adopted for ^{55}Mn .

No.	Type	Quantity	Default	Adopted
1	Single resonance	$\text{corr}(\Gamma_n, \Gamma_\gamma)$	0.0	0.0
2	Resonance-resonance	$\text{corr}(\Gamma_{\gamma 1}, \Gamma_{\gamma 2})$	0.5	0.5
3	Resonance-resonance	$\text{corr}(\Gamma_{n1}, \Gamma_{n2})$	0.5	0.5
4	Resonance-resonance	$\text{corr}(\Gamma_{n1}, \Gamma_{\gamma 2})$	0.0	0.0
5	Pot. scattering-resonance	$\text{corr}(R', \Gamma_n)$	-0.5	-0.5
6	Bin-bin	$\text{corr}(\bar{\sigma}_{\gamma 1}, \bar{\sigma}_{\gamma 2})$	0.5	0.5
7	Bin-bin	$\text{corr}(\bar{\sigma}_{n1}, \bar{\sigma}_{n2})$	0.5	0.5
8	Thermal-resonance	$\text{corr}(\sigma_\gamma^{th}, \bar{\sigma}_\gamma)$	0.0	0.0
9	Thermal-resonance	$\text{corr}(\sigma_n^{th}, \bar{\sigma}_n)$	0.0	0.0
10	Cross-correlation	$\text{corr}(\sigma_n^{th}, \sigma_\gamma^{th})$	0.0	0.0
11	Cross-correlation	$\text{corr}(\sigma_n^{res}, \sigma_\gamma^{res})$	-0.5	0.0

Table 8.7: Uncertainties of integral quantities (thermal cross sections and resonance integrals) for ^{55}Mn . Compared are values computed from our covariance matrices and those given in Atlas of Neutron Resonances.

Quantity	Present	Atlas	Comment
Capture thermal	0.8%	0.37%	We adopted 0.8%, see Table 8.1
Capture RI	3.3%	3.7%	
Elastic thermal	3.0%	1.5%	We adopted 3.0%, see Table 8.1
Elastic RI	2.4%	-	

- Uncertainties of integral quantities. Our results are compared with values in Atlas in Table 8.7. Uncertainties of our cross sections are higher than the values given in Atlas as explained in Table 8.1. Resonance integrals were computed by integrating over the energy range 0.5 eV - 208 keV, *i.e.* up to the upper end of the resonance region. Agreement with Atlas for capture is pretty good, uncertainty for elastic is not provided in Atlas as no experimental values are available.

For completeness and future reference we write down explicit expressions for resonance integrals. Usual resonance integral

$$RI = \int_{0.5\text{eV}}^{E_0^{\text{max}}} \frac{1}{E} \sigma(E) dE \quad (8.1)$$

should be computed as summation over small energy bins. Considering our course bin structure and related average cross sections one can write

$$RI = \sum_i RI_i \approx \sum_i \frac{1}{E_i^{\text{eff}}} \bar{\sigma}(E_i) \Delta E_i, \quad (8.2)$$

where the effective energy for each bin, E_i^{eff} , must be suitably determined since $1/E$ is rapidly changing function. This is done as follows. Assume energy bin with boundaries E_i and E_{i+1} , then effective energy is defined as the point which splits the bin so that contribution from E_i to E_i^{eff} is the same as from E_i^{eff} to E_{i+1} ,

$$\begin{aligned} \int_{E_i}^{E_i^{\text{eff}}} \frac{1}{E} &= \int_{E_i^{\text{eff}}}^{E_{i+1}} \frac{1}{E}, \\ \ln \frac{E_i^{\text{eff}}}{E_i} &= \ln \frac{E_{i+1}}{E_i^{\text{eff}}}, \\ E_i^{\text{eff}} &= \sqrt{E_i E_{i+1}}. \end{aligned} \quad (8.3)$$

Resonance integral uncertainty is obtained by quadratic summation of contributions from individual bins taking into account both diagonal terms and off-diagonal terms of the covariance matrix. Making use of relative uncertainty of average cross section of a given bin, $\Delta \bar{\sigma}(E_i)$, one gets

$$\Delta RI_i = \frac{1}{E_i^{\text{eff}}} \Delta \bar{\sigma}(E_i) \Delta E_i \quad (8.4)$$

and finally

$$(\Delta RI)^2 = \sum_{i,j} \text{corr}(i, j) \Delta RI_i \Delta RI_j = \sum_i (\Delta RI_i)^2 + 2 \sum_{i < j} \text{corr}(i, j) \Delta RI_i \Delta RI_j. \quad (8.5)$$

One should keep in mind that bins in the thermal region are fully correlated, there is no correlation between thermal and resonance region, and correlation between energy bins in the resonance is region is 0.5.

Chapter 9

Conclusions

We developed a formalism for producing MF33 covariances in the resonance region based on the kernel approximation for capture and elastic scattering and using data from the Atlas of Neutron Resonances. Extension to fission should be straightforward. The formalism is transparent and based on analytical expressions.

Practical application of this formalism was illustrated on covariances for ^{55}Mn . The formalism works well in particular for capture and the results look plausible, though one has to keep in mind that the outcome depends on the choice of resonance-resonance correlations. These are not well known and one has to resort on estimates driven by general considerations. Contribution from potential scattering to uncertainty budget of elastic scattering cross sections is significant in particular at high resonance energies. Our results were compared with an alternative MF32 approach, showing good agreement in capture covariances and issues of MF32 approach in elastic scattering.

Comparison with recent ^{55}Mn evaluation (2008) included in ENDF/A suggested that there are several issues in the current ENDF/A file. In addition this comparison confirmed issues in processing MF32 files as seen on not negligible differences between $^{55}\text{Mn}(n,\gamma)$ uncertainties produced by the most recent versions of NJOY and PUFF.

In the near future our new procedure should be applied to Cr-Fe-Ni structural materials which are almost pure scatterers and are priority materials for reactor applications. Other candidates should include troublesome materials in ENDF/B-

VII.0, primarily ^{89}Y , followed by $^{191,193}\text{Ir}$ and possibly also $^{156,158}\text{Gd}$. Extension to fission and testing with a suitable actinide should be pursued as well.

Acknowledgments

This work has been performed under AFCI covariance data project sponsored by DOE-NE. It was also part of ARRA project of developing neutron cross section covariances for ENDF/B-VII library sponsored by DOE-SC. This sponsorship is gratefully acknowledged. One of us (YSC) is grateful to the NNDC for warm hospitality. The authors are grateful to M. Herman and M. Pigni for numerous discussions on covariances. They wish to thank R. Arcilla for his assistance with processing.

Brookhaven National Laboratory is sponsored by the Office of Nuclear Physics, Office of Science of the U.S. Department of Energy under Contract No. DE-AC02-98CH10886 with Brookhaven Science Associates, LLC.

Bibliography

- [1] S.F. Mughabghab, “Atlas of Neutron Resonances: Thermal Cross Sections and Resonance Parameters”, Elsevier Publisher, Amsterdam, 2006.
- [2] M. Herman, S.F. Mughabghab, P. Obložinský, M. Pigni, D. Rochman, “Neutron Cross Section Covariances in the Resolved Resonance Region”, Brookhaven National Laboratory, Report BNL-80173-2008, June 2008.
- [3] S.F. Mughabghab, private communication, 2009.
- [4] J.D. Smith III, “Processing ENDF/B-V Uncertainty into Multigroup Covariance Matrices”, Oak Ridge National Laboratory, Report ORNL/TM-7221, June 1980.
- [5] D. Wiarda and M.E. Dunn, “PUFF-IV: A Code for Processing ENDF Uncertainty Data into Multigroup Covariance Matrices”, Oak Ridge National Laboratory, Report ORNL/TM-2006/147 (2006).
- [6] F.H. Fröhner, “Evaluation of Resonance Parameter Covariances and Cross Section Fluctuations for Structural Materials”, JEFF/DOC-463 (NEA, Paris 1993).
- [7] F.H. Fröhner, “On Uncertainty Evaluation and Fluctuations in the Resolved and Unresolved Resonance Regions”, Proc. Int. Conf on Nuclear Data for Science and Technology (Gatlinburg, May 9-13, 1994), ed. J.K. Dickens, American Nuclear Society 1994, p.597.
- [8] F.H. Fröhner, “Reevaluation of the Resolved Resonance Parameters for $^{56}\text{Fe}+n$ Including Uncertainties and Correlations”, JEFF/DOC-574 (NEA, Paris 1995).

- [9] R.E. McFarlane and D.W. Muir, “The NJOY Nuclear Data Processing System, Version 91”, Los Alamos National Laboratory, Report LA-12740-M (1994); see p.III-9.
- [10] F.H. Fröhner, “Evaluation and Analysis of Nuclear Resonance Data”, JEFF Report 18 (OECD NEA, Paris 2000), p.56.
- [11] M. Herman and A. Trkov (editors), “ENDF-6 Formats Manual: Data Formats and Procedures for the Evaluated Nuclear Data File ENDF/B-VI and ENDF/B-VII”, Brookhaven National Laboratory, Report BNL-90365-2009 (CSEWG Document ENDF-102), June 2009, p. 317.
- [12] M.B. Chadwick, P. Obložinský, M. Herman *et al*, “ENDF/B-VII.0: Next Generation of Evaluated Nuclear Data Library for Nuclear Science and Technology”, Nuclear Data Sheets **107** (2006) 2931.
- [13] B. Pritychenko and A.A. Sonzogni, “Sigma: Web Retrieval Interface for Nuclear Reaction Data”, Nuclear Data Sheets **109** (2008) 2822.
- [14] P. Obložinský, C.M. Mattoon *et al*, “Progress on Nuclear Data Covariances: AFCI-1.2 Covariance Library”, Brookhaven National Laboratory Report BNL-90897-2009, December 2009.
- [15] M. Williams, “Generation of Approximate Covariance Data”, Oak Ridge National Laboratory, unpublished note dated August 12, 2004.
- [16] JEFF Team, “The JEFF-3.0 Nuclear Data Library”, JEFF Report 19 (OECD, Nuclear Energy Agency, Paris 2005).
- [17] R.C. Little *et al*, “Low-fidelity Covariance Project”, Nuclear Data Sheets **109** (2008) 2828.
- [18] M. Herman, R. Capote, B. Carlson *et al*, “EMPIRE: Nuclear Reaction Model Code System for Data Evaluation”, Nuclear Data Sheets **108** (2007) 2655.
- [19] C.M. Mattoon, “Issues in the Resolved Resonance Region in ^{55}Mn Covariances”, Covariance Workshop, Port Jefferson, USA, June 23, 2009, unpublished.

- [20] H. Derrien, L.C. Leal, N.M. Larson, K. Guber, D. Wiarda, G. Arbanas, "Neutron resonance parameters of ^{55}Mn from Reich-Moore analysis of recent experimental neutron transmission and capture cross sections", Inter. Conf. on the Physics of Reactors (PHYSOR), Interlaken, Switzerland, September 1-14, 2008.
- [21] M. Herman, M.T. Pigni, P. Obložinský, S.F. Mughabghab, C.M. Mattoon, R. Capote, Young-Sik Cho, A. Trkov, "Development of Covariance Capabilities in EMPIRE Code", Nuclear Data Sheets **109** (2008) 2752.
- [22] S.-Y. Oh, J. Chang, S.F. Mughabghab, "Neutron Cross Section Evaluations of Fission Products Below the Fast Neutron Energy Region, Brookhaven National Laboratory, Report BNL-NCS-67469, April 2000.
- [23] H. Derrien, L.C. Leal, N.M. Larson, K. Guber, D. Wiarda, G. Arbanas, "Evaluation of the resonance parameters of Mn-55 in the energy range 0 to 122 keV", file submitted to ENDF/A in fall 2008, retrieved from the NNDC GForge server on April 6, 2010.
- [24] A.D. Carlson, V.G. Pronyaev, D.L. Smith *et al*, "International Evaluation of Neutron Cross Section Standards", Nuclear Data Sheets **110** (2009) 3215.